

Jostein Ertsås

Assessing the impact of CaO addition to pH, alkalinity and inorganic carbon in seawater with special focus on the kinetics

Evaluation of artificial ocean alkalinisation

Master's thesis in Environmental Chemistry

Supervisor: Murat Van Ardelan

May 2019

Jostein Ertsås

Assessing the impact of CaO addition to pH, alkalinity and inorganic carbon in seawater with special focus on the kinetics

Evaluation of artificial ocean alkalisation

Master's thesis in Environmental Chemistry
Supervisor: Murat Van Ardelan
May 2019

Norwegian University of Science and Technology
Faculty of Natural Sciences
Department of Chemistry



Norwegian University of
Science and Technology

Abstract

Ocean liming, OL is proposed as a geoengineering technic with the intention to artificial increase ocean alkalisation. Enhanced alkalinity will increase the acid neutralizing capacity and thereby reverse ocean acidification. The increased alkalinity is predicted to originate from CO₂, making OL a tool to sequester atmospheric CO₂. This study tries to clarify the mechanisms taking place in OL by measuring pH, total alkalinity, particular formation and actual ions development using two types of CaO (coarse and fine). From comparing rate for different concentrations of fine CaO (0.01-, 0.015- and 0.02 g L⁻¹) the reaction rate appears to follow first order. The extent of particular formation which unfolds the first 10-20 minutes after an addition is related to CaO dose. The magnitude of the formation could be important in OL contexts as it might cause biological consequences. The absolute pH and alkalinity for different grain size CaO is comparable, but coarse grained showed a slower reaction rate and only a small immediate peak of precipitation. Total alkalinity increased 1.68 mole per mole CaO (0.01 g L⁻¹ fine CaO), but OL potential to sequester CO₂ should be investigated further in an open system experiment with constant pCO₂. OL's global contribution in removing CO₂ is however closely linked to the scale of production as well as carbon capture technologies, emissions from mining, transportations and heating. OL can however be a possible solution to reverse ocean acidification.

Sammendrag

Ocean Liming, OL er en foreslått teknologi der havet får mer alkalinitet fra tilførsel av CaO. Økt alkalinitet vil forsterke havets evne til å nøytralisere syre og dermed reversere havforsuring. Alkalinitet er sterkt knyttet til havets beholdning av uorganisk karbon og dens økte verdi forventes å komme fra atmosfærisk CO₂. Denne studien ønsker å bedre forståelsen av mekanismene tilknyttet OL ved å måle pH, total alkalinitet, partikkelformasjon og utviklingen av ioner i løsning ved å studere to typer CaO (grov- og finkornet). Ved å sammenligne reaksjonshastigheten av forskjellige CaO-konsentrasjoner (0,01-, 0,015- og 0,02 g L⁻¹) tyder det på at reaksjonen følger første orden. Omfanget av partikkelformasjon som inntreffer de første 10-20 minuttene er relatert til mengde CaO tilført. Grad av partikkelformasjon som inntreffer er viktig i en OL-sammenheng da det kan føre til biologiske konsekvenser. Den totale endringen i pH og alkalinitet er sammenlignbar for forskjellige typer CaO, men den grovkornede reaksjonshastigheten er langsommere og danner kun i liten grad partikler de første 10-20 minuttene. Total alkalinitet økte 1,68 mol per mol CaO tilført (0,01 g L⁻¹ fin CaO), men potensialet for OL til å isolere CO₂ i havet bør undersøkes i sammenheng med konstant pCO₂. OL sitt globale bidrag til å fjerne CO₂ i atmosfæren er imidlertid tett knyttet til mengde CaO anvendelig, samt karbonfangstteknologi, utslipp fra gruvedrift, transport og oppvarming. OL kan imidlertid være en mulig løsning til å reversere havforsuring.

Acknowledgements

I thank the chemistry department at the Norwegian University of Science and Technology in Trondheim for founding this study. I am grateful to my supervisor, Murat Van Ardelan introducing me to the subject and providing needed guidance. Big thanks also to Nicolas Sanchez for helping me around the laboratory. I would also like to thank Kjersti Andresen from Trondheim Biological Station and Syverin Lierhagen from the department of chemistry for analysing and helping with my samples. I am also thankful to Kjell Reidar Kvam and Martin Mengede from Miljøkalk AS providing the different types CaO used in this study. Finally, I will thank my loving partner, Kristine Henriksen providing feedback and taking care of our life back home. I would not be able to complete this master's degree without your patient.

Table of contents

| | |
|---|--------|
| Abstract..... | p.i |
| Sammendrag..... | p.ii |
| Acknowledgements..... | p.iii |
| Table of contents..... | p.iv |
| List of tables..... | p.vi |
| List of figures | p.vii |
| List of abbreviations | p.viii |
| | |
| 1. Introduction..... | p.1 |
| 1.1 Introduction..... | p.1 |
| 1.2 Inorganic carbon..... | p.2 |
| 1.3 Definition of alkalinity..... | p.4 |
| 1.4 Changes in alkalinity..... | p.7 |
| 1.5 State of saturation..... | p.8 |
| 1.6 Artificial ocean alkalisation..... | p.9 |
| 1.7 Lime cycle..... | p.10 |
| 1.8 Complementary research | p.12 |
| 1.9 Ionic strength and activity..... | p.13 |
| 1.10 Finding pH..... | p.14 |
| 1.11 Kinetics..... | p.15 |
| 1.12 Scope and calculation | p.17 |
| 2. Material and method..... | p.18 |
| 2.1 CaO..... | p.18 |
| 2.2 Seawater..... | p.18 |
| 2.3 pH calibration..... | p.19 |
| 2.4 Test to find right dose of CaO..... | p.20 |
| 2.5 Alkalinity and pH..... | p.20 |
| 2.6 Activity coefficient and alkalinity calculation..... | p.21 |
| 2.7 Filtrations..... | p.21 |
| 2.8 Preparation, analysing and DIC calculation..... | p.22 |
| 3. Results..... | p.24 |
| 3.1 Test result to find right dose CaO for main experiment..... | p.24 |
| 3.2 Results from fine and coarse grained CaO..... | p.25 |

| | |
|---|------|
| 3.2.1 pH, alkalinity for fine grained CaO..... | p.25 |
| 3.2.2 pH, alkalinity for coarse grained CaO..... | p.27 |
| 3.3 Results from different concentrations of CaO..... | p.29 |
| 3.3.1 Effect on pH from different concentrations of CaO..... | p.29 |
| 3.3.2 ICP-MS of filtrate..... | p.31 |
| 3.3.3 Particulate inorganic carbon formation..... | p.33 |
| 3.4 Duplicate XRF runs..... | p.37 |
| 4. Discussion..... | p.39 |
| 4.1 Feedback on pH from different CaO addition..... | p.39 |
| 4.2 Kinetic interpretations..... | p.40 |
| 4.3 Alkalinity and DIC | p.42 |
| 4.4 Dissolution and precipitation..... | p.43 |
| 4.5 Limitations, challenges and further investigations..... | p.45 |
| 4.6 Conclusion..... | p.47 |
| References | p.48 |
| Appendix..... | p.53 |
| A Internal and external pH measurements + dataset..... | p.53 |
| B Dataset for alkalinity and CO ₂ sys calculation..... | p.55 |
| C Data gathered by NITON XRF Analyzer..... | p.57 |
| D ICP-MS dataset and Ca/Mg correlation..... | p.58 |
| E Dataset from PIC determination..... | p.60 |
| F Analyse-report AR-MKA-17-0030..... | p.63 |

List of tables

| | |
|--|------|
| Table 1: All the species contributing to alkalinity..... | p.5 |
| Table 2: Reaction order | p.16 |
| Table 3: Changes in alkalinity species after $\sim 0.01 \text{ g L}^{-1}$ fine CaO addition..... | p.26 |
| Table 4: Changes in alkalinity species after $\sim 0.01 \text{ g L}^{-1}$ coarse CaO addition..... | p.28 |
| Table 5: Final calcium concentration..... | p.45 |

List of figures

| | |
|--|------|
| Figure 1: Bjerrum plot for the carbonate system..... | p.3 |
| Figure 2: Species contribution to alkalinity..... | p.5 |
| Figure 3: Major cations and anions in seawater..... | p.6 |
| Figure 4: Overview of changes to total alkalinity and dissolved inorganic carbon..... | p.8 |
| Figure 5: Overview of Trondheimsfjorden inlet and TBS..... | p.19 |
| Figure 6: pH changes from increasing amount of CaO..... | p.24 |
| Figure 7: pH values after $\sim 0,01 \text{ g L}^{-1}$ fine CaO mixed in seawater..... | p.25 |
| Figure 8: pH values after $\sim 0.01 \text{ g L}^{-1}$ coarse CaO mixed in seawater..... | p.27 |
| Figure 9: pH/alkalinity change from coarse and fine $\sim 0.01 \text{ g L}^{-1}$ CaO..... | p.29 |
| Figure 10: Precipitate after end of experiment..... | p.30 |
| Figure 11: pH variation from three concentration fine-CaO in seawater..... | p.31 |
| Figure 12: [Ca] and [Mg] after addition of $\sim 0.01 \text{ g L}^{-1}$ coarse grained CaO..... | p.31 |
| Figure 13: [Ca] and [Mg] after addition of $\sim 0.01 \text{ g L}^{-1}$ fine grained CaO..... | p.32 |
| Figure 14: [Ca] and [Mg] after addition of $\sim 0.015 \text{ g L}^{-1}$ fine grained CaO..... | p.32 |
| Figure 15: [Ca] and [Mg] after addition of $\sim 0.02 \text{ g L}^{-1}$ fine grained CaO..... | p.33 |
| Figure 16: Calcium trends in solution after different CaO additon..... | p.33 |
| Figure 17: Particulate carbon after $\sim 0.01 \text{ g L}^{-1}$ coarse CaO addition..... | p.34 |
| Figure 18: Particulate carbon after $\sim 0.01 \text{ g L}^{-1}$ fine CaO addition..... | p.35 |
| Figure 19: Particulate carbon after $\sim 0.015 \text{ g L}^{-1}$ fine CaO addition..... | p.36 |
| Figure 20: Particulate carbon after $\sim 0.02 \text{ g L}^{-1}$ fine CaO addition..... | p.36 |
| Figure 21: Comparison of particulate carbon formation from different grain and concentration of CaO..... | p.37 |
| Figure 22: XRF solid Ca after $\sim 0.01 \text{ g L}^{-1}$ CaO addition (trial A)..... | p.38 |
| Figure 23: XRF solid Ca after $\sim 0.01 \text{ g L}^{-1}$ CaO addition (trial A)..... | p.38 |
| Figure 24: Changes in $[\text{OH}^-]$ from different concentrations of CaO | p.41 |
| Figure 25: Comparing rates of formation from three doses of CaO..... | p.41 |

List of abbreviations

| | |
|-------------|--|
| AOA | Artificial Ocean Alkalinisation |
| $B(OH)_4^-$ | Tetrahydroxyborate |
| Ca | Calcium |
| $CaCO_3$ | Calcium carbonate |
| CaO | Calcium Oxide, Quicklime, Burnt Lime |
| $Ca(OH)_2$ | Slaked Lime, Hydrated Lime |
| CCS | Carbon Capture and Storage |
| CH_4 | Methane |
| CO_2 | Carbon Dioxide |
| pCO_2 | Partial Pressure of Carbon Dioxide |
| CO_3^{2-} | Carbonate |
| DOC | Dissolved Organic Carbon |
| DIC | Dissolved Inorganic Carbon |
| GFF | Glass Fibres Filter |
| H^+ | Proton |
| HCO_3^- | Bicarbonate |
| HCl | Hydrogen chloride |
| HDPE | High-density polyethylene |
| ICP-MS | inductively coupled plasma mass spectrometry |
| Mg | Magnesium |
| $MgCO_3$ | Magnesium Carbonate |
| MgO | Magnesium Oxide |
| NBS | National Bureau of Standards buffer scale |
| OH^- | Hydroxide |
| OL | Ocean Liming |
| POC | Particular Organic Carbon |
| PIC | Particular Inorganic Carbon |
| ppm | parts per million |
| TA | Total Alkalinity |
| TBS | Trondheim's Biological Station |
| XRF | X-ray fluorescence |
| [Element] | Concentration of actual element |

1. INTRODUCTION

1.1 Introduction

From ice core records and observations there are unequivocal evidence that greenhouse gases such as carbon dioxide (CO₂), methane (CH₄) and nitrous oxide (N₂O) have increased over the last centuries (Chen, Frame, Mahowald & Winther 2013). This is causing a heating effect, changing the earth's complex systems in the atmosphere and in the ocean. From the greenhouse gases, CO₂ accounts for at least half of the greenhouse effect that causes this global warming, even though the anthropogenic source for CO₂ is small compared to the exchange of natural CO₂ (Gupta & Fan 2002). The total amount that has been liberated from natural reservoirs increased the concentration of CO₂ in the atmosphere from 280 ppm, before the industrial revolution, to 355 ppm in 1990 (Gupta & Fan 2002). In May 3, 2019, the number has been measured to 413.52 ppm by Mauna Loa Observatory in Hawaii, increased from 410.30 ppm measured the same date last year (Keeling et al. 2019). This will not account for all the extra anthropogenic emissions released, since the ocean will absorb one quarter of the total CO₂ that emits into the atmosphere each year (Ma, You, Ji, Ma & Li 2015).

The CO₂ that is dissolved in oceans and other waters, changes the aquatic chemistry by lowering the pH (Chen et al. 2013). This process when pH decrease is generally called acidification and is one of the mayor threats, known and unknown to serval organisms in different ecosystems (Ma et al. 2015). The average ocean pH has approximately decreased from 8.2 to 8.1 since the beginning of the industrial revolution (Hansson & Gattuso 2011). This number could change more drastically regionally and in different depth. At current pH we find at least 90 % of inorganic carbon in the carbon cycle staying in the [HCO₃⁻] form, and less than 10 % will be found as [CO₃²⁻]. In decreasing pH caused by more acidic water even lower amount of carbonate will exist naturally (Riebesell, Fabry, Hansson & Gattuso 2010). Many organisms in the ocean are dependent on the ability to make carbonate shells and skeletons; specially mussels, corals and sea urchins. Lowering available CO₃²⁻ is predicted to decrease calcification for these species (Rafferty 2011). Coral reefs are considered especially vulnerable and models predict that skeletal density will decrease 20,3 % by 2100 (Mollica et al. 2018). This is not the case for all oceanic organisms, but a meta study found that 57 % of echinoderms and 50 % and molluscs were negatively affected at pCO₂

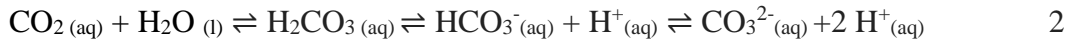
levels between 500 and 650 ppm (Feng, Koeve, Keller & Oschlies 2017). Non-calcifying organisms may also be affected as acidification can reduce their metabolic rates or damage their larva or juvenile stages (Frommel et al. 2011; Rosa & Seibel 2008). Though the evolvement of some phytoplankton might suffer under acidic conditions; carbon enrichment can also be a source for photosynthetic organisms boosting their growth (Connell et al 2017). The entire food chain in the ocean is based on the production of phytoplankton, and an increase or decrease in their formation could have widespread consequences. Different conditions will give different feedback and would at least lead to a shift in composition of species (Yamamoto-Kawai, McLaughlin, Carmack, Nishino & Shimada 2009).

This process of acidification has increased by 30 % over the last 150 years and a big uncertainty arises about the absolute effect of the current and rising $[\text{CO}_2]$, that is unmatched in the earth's past 20 million years (Ma et al. 2015; Rafferty 2011). In their projections about the future, the international energy agency (IEA, 2017) showed growing energy demand that will make it even harder to shift the usage of fossil fuels. In the same projections it is believed that oil demand will continue to rise until 2040 (IEA, 2017). Effort to decrease $p\text{CO}_2$ in the atmosphere and reverse acidification in the oceans may therefore be necessary on a global or local scale.

Motivation for this study is based on the urgency to understand the complicity in oceanic carbon reservoir and exchanges between the systems. Assessing the basic mechanism of the proposed geoengineering solution, where we actively interfere in carbon exchange using CaO to artificially increase the ocean alkalinity. Great amount of understanding is necessary to be able to take a responsible choice and hopefully this thesis can present current knowledge and unfold new information for this little discussed geoengineering technique.

1.2 Inorganic carbon

Carbon species constantly change when it goes through metabolism and natural chemical processes and are present in marine system as inorganic or organic (Ma et al. 2015). Organic forms of carbon (POC and DOC) are basically biogenic materials (not an issue for this study) while inorganic carbon is mainly present as particulate (i.e carbonate minerals) and dissolved form (DIC, dissolved inorganic carbon) (M. V. Ardelan, personal communication, April 28, 2019). DIC, presented as HCO_3^- , CO_3^{2-} and $\text{CO}_2(\text{aq})$ is in an equilibrium condition with atmospheric $\text{CO}_2(\text{g})$.



The inorganic carbon species in aquatic carbon cycle can be determined by pH and the total alkalinity (TA) of seawater (M. V. Ardelan, personal communication, April 28, 2019). The species will change dependent on the pH. At low pH, below 6, there will be an abundance of $[\text{H}_2\text{CO}_3^*]$ and small $[\text{HCO}_3^-]$ while $[\text{CO}_3^{2-}]$ will be close to zero. $[\text{H}_2\text{CO}_3^*]$ meaning $[\text{CO}_2] + [\text{H}_2\text{O}]$ together with 0.03-1 % of $[\text{H}_2\text{CO}_3]$; since the reaction between them is too fast and their relative proportions are difficult to determine analytically it is more practical to put these concentrations together (Stumm & Morgan 1996). While at high pH, over 9.5, there is abundant of $[\text{CO}_3^{2-}]$ and smaller $[\text{HCO}_3^-]$ and close to zero $[\text{H}_2\text{CO}_3^*]$. In between pH 6 and pH 9.5 $[\text{HCO}_3^-]$ dominate.

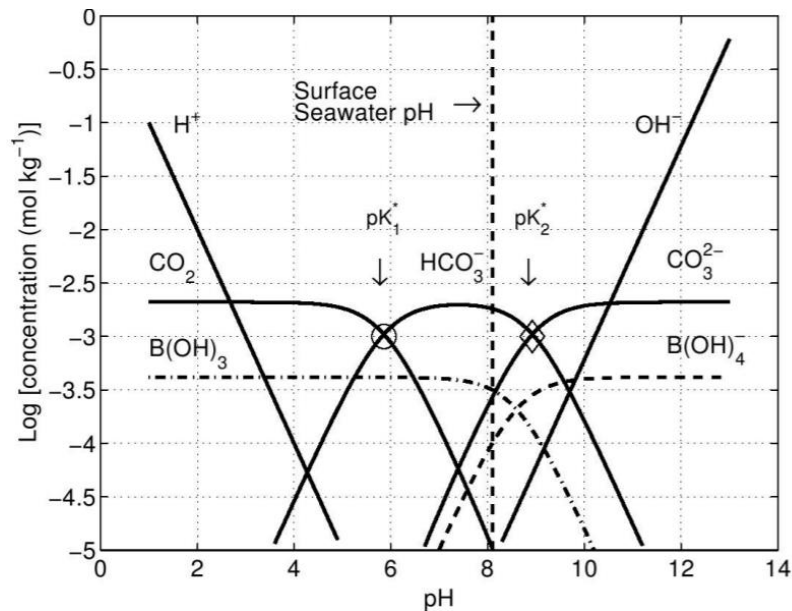


Figure 1 Bjerrum plot for the carbonate system: Composition of DIC species change when pH changes in a closed system. Oceanic average pH is ~8.1, which result in ~1 % CO₂, ~90 % HCO₃⁻ and 9 % CO₃²⁻ (Völker 2015).

The pK dependent on the specific temperature, pressure and salinity and a shift in these parameters will lead to a change in the proportion between $[\text{H}_2\text{CO}_3]$, $[\text{HCO}_3^-]$ and $[\text{CO}_3^{2-}]$ (Zeebe & Wolf-Gladrow 2001). A decrease of temperature and salinity leads to higher pK as does higher pressure. The same is true for the dissociation constant for water, pK_w, meaning the proportion of CO_3^{2-} will be lower in saltwater than freshwater.

1.3 Definition of alkalinity

Alkalinity, or total alkalinity, can represent the acid neutralizing capacity in an aquatic system which illustrate the oceans ability to work as a buffer (Stumm & Morgan 1996). Thus, an increase in alkalinity means an increase in bases capable of absorbing acid, $[H^+]$ (González & Ilyina 2016). Without this buffer ability the acidification of the oceans would be more substantial. There are many definitions of alkalinity, but Dicksons definition is regarded as one of the more precise: *“The total alkalinity of a natural water is thus defined as the number of moles of hydrogen ion equivalent to the excess of proton acceptors (bases formed from weak acids with a dissociation constant $k \leq 10^{-4.5}$, (at 25 °C and zero ionic strength) over protons donors (acids with $k > 10^{-4.5}$) in one kilogram of sample”* (Dickson 1981, p. 611). This definition has a separation of proton acceptors and proton donors at a chosen value of pH 4,5 where all the bases of interest have protonated to the zero level species, though thoughtfully chosen, is arbitrary. In aquatic systems you may wish to include all components contributing to the alkalinity, but many aquatic systems contain several species with a neglectable contribution. This is the case for seawater for pH around 8,2 in contrast to aquatic systems with low pH which many of the components have an increasingly important contribution (Zeebe & Wolf-Gladrow 2001; Stumm & Morgan 1996). This neglectable contribution is due to carbonate alkalinity makes up most of the total alkalinity. In natural environment, the product of the highly occurring, weathered carbonate rocks and the presence of CO_2 in the atmosphere is an immense contributor and overshadows most of the other sources. The biggest contributor after carbonate species is $B(OH)_4^-$ and water itself, which is small in comparison to carbonate, but is still in so large concentration it should not be excluded when measuring a natural environment (Zeebe & Wolf-Gladrow 2001; Stumm & Morgan 1996). In this thesis with pH values around 8, the alkalinity is therefore expressed for most practically purposes by:

$$TA = [HCO_3^-] + 2[CO_3^{2-}] + [B(OH)_4^-] + [OH^-] - [H^+] \quad 3$$

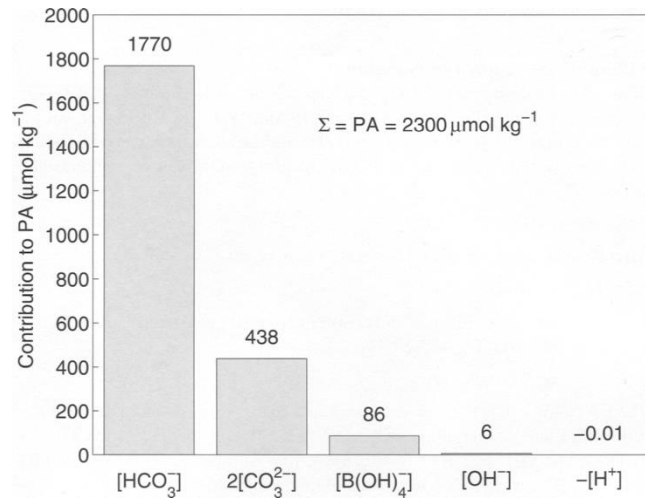


Figure 2 Species contribution to alkalinity: expected contribution with TA (equation 3)= 2300 μmol kg⁻¹, DIC = 2000 μmol kg⁻¹, T =25 oC and salinity =35 (Zeebe & Wolf-Gladrow 2001).



In equation 5 we can see CO_3^{2-} contribute with two-unit alkalinity because it has the ability to absorb two protons from the solution above the chosen pH 4.5, which defines the zero level of protons, H_2CO_3 (Stumm & Morgan 1996).

Table 1: All the species contributing to alkalinity. Negative ions will contribute to TA positively, while H^+ contribute negatively (Stumm & Morgan 1996; Zeebe & Wolf-Gladrow 2001).

| Species contributing to alkalinity |
|---|
| HCO_3^- , CO_3^{2-} , HS^- , S_2^{2-} , H_3SiO_4^- , $\text{H}_2\text{SiO}_4^{2-}$, B(OH)_4^- , org^- , HPO_4^{2-} , PO_4^{3-} , HSO_4^- , H^+ |

The concept of alkalinity is closely linked to the charged balance in seawater. By assuming that the ocean is balanced in regard to negative and positive ions, we can derive total alkalinity by the small charge imbalance between the mayor cations and mayor anions. This imbalance is compensated by mainly anions from carbonic acids, and even though it is a small amount in comparison to other components in the ocean, it is the reason for 39 000 gigatons inorganic carbon stored in the ocean (Stumm & Morgan 1996).

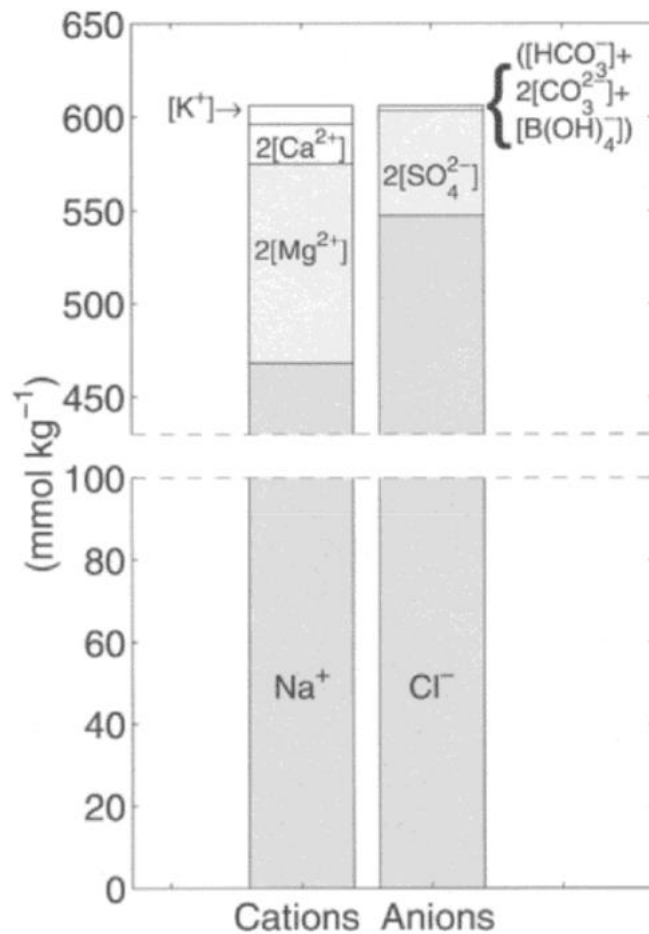


Figure 3 Major cations and anions in seawater: List of the concentration and charge balance of major cations and anions in a seawater sample with salinity 35. The difference between the yields of anions and cations is equal to the total alkalinity in seawater, if you disregard the alkalinity contribution from uncharged species (Zeebe & Wolf-Gladrow 2001).

Alkalinity can be found by titrating a solution with a strong acid, like HCl which dissociates completely into H⁺ and Cl⁻ (Zeebe & Wolf-Gladrow 2001). The proton will combine with bases to form their conjugated acid. Addressing carbonate species, CO₃²⁻ will initially decrease and HCO₃⁻ increase. As titration continue, HCO₃⁻ will also decrease, as it converts to CO₂. In the end, when HCO₃⁻ is almost completely converted to CO₂, the amount of added acid up to a specific end point will be equal to initial alkalinity (Zeebe & Wolf-Gladrow 2001).

1.4 Changes in alkalinity

Units of alkalinity, (Eq L^{-1}), is mostly a conservative quantity, as it is expressed based on the charge balance of the major ions that are unaffected by changes in temperature or pressure in natural environment (Zeebe & Wolf-Gladrow 2001). However, it has been shown that alkalinity can be inversely proportional to sea surface temperature as a consequence of upwelling zones. For instances, it will increase with higher latitudes and depths (Millero, Lee & Roche 1998). The equilibrium constant is additionally prone to alteration as temperature and pressure change and thereby cause small feedback to the total alkalinity (Clark 2013). Higher temperature increases the CO_3^{2-} to HCO_3^- ratio. At the same time the proton concentration increases slightly forcing a lower pH. Meaning a warmer solution have a better buffer capacity even though it has a lower pH (AWC 2019). Partial pressure of CO_2 , $p\text{CO}_2$ in the atmosphere have increased in recent years and will continue in the near future, mostly due to burning of fossil fuel. It causes pH changes but are not in any significantly way altering the alkalinity of surface ocean (Stumm & Morgan 1996; Millero et al. 1998). The surface ocean is oversaturated in respect to CaCO_3 and we can therefore disregard any heterogenous reaction of the seawater with CaCO_3 , and alkalinity consequently stay constant.

There are several processes that lead to changes in alkalinity. Some minor changes to alkalinity happen as a consequence of metabolic processes like photosynthesis, respiration, nitrification, denitrification, sulphide oxidation and sulphate reduction that are mediated by oceanic organisms (Stumm & Morgan 1996). Even though CO_2 do not contribute to total alkalinity by itself, NO_3^- , NH_4^+ and HPO_4^{2-} is assimilated in photosynthesis and respiration and are accompanied by the uptake of H^+ or OH^- . When algae use 1 mol of NO_3^- , assuming that electroneutrality is ensured, it need a parallel uptake of H^+ or release of OH^- , thus increasing total alkalinity by 1 mol. Factors that lead to more major changes in total alkalinity are evaporation, precipitation, input of “fresher” waters and the formation and melting of ice. The level of salinity is therefore closely linked with total alkalinity. Thus, a dilution of a sample will change the alkalinity, while pH remain the same (Zeebe & Wolf-Gladrow 2001; Stumm & Morgan 1996). Biogenic precipitation of CaCO_3 by marine organisms or dissolution of calcareous shells or skeletons are a major natural contributor to change in alkalinity. Precipitation leads to a decrease of Ca^{2+} , thus decreasing the charge difference between the ions in the ocean and lowering the alkalinity (Zeebe & Wolf-Gladrow 2001). Dissolution of CaCO_3 would instead reverse this reaction and enhance the oceans ability to withstand acidification and to store more carbon. Precipitation of carbonate minerals can also

occur abiotically which is of major importance in this study and is discussed further in the next section. From precipitation of 1 mole carbonate mineral, the ocean will lose 1 mole DIC and 2 mole total alkalinity, as can be seen in equation 6.



1.5 State of saturation

In natural water this reaction depends on the state of saturation. Saturation is determined as, $\Omega = [\text{Ca}^{2+}][\text{CO}_3^{2-}]/K_{\text{sp}}$ (the solubility product). In open ocean the K_{sp} is mostly determined by the CO_3^{2-} , as variation of $[\text{Ca}^{2+}]$ is rather small and closely related to the salinity (Zeebe & Wolf-Gladrow 2001). When saturation is above 1 we have an oversaturated solution where free Ca^{2+} and CO_3^{2-} can react and form CaCO_3 . When saturation is below 1 it is undersaturated meaning no more CaCO_3 will form (Ilyina, Wolf-Gladrow, Munhoven & Heinze 2013). Rather, CaCO_3 already existing in undersaturated conditions will tend to dissolve into Ca^{2+} and CO_3^{2-} . While a CaCO_3 sink would alter the total carbon in circulation, a dissolution would lead to an increase in alkalinity (González & Ilyina 2016). CO_3^{2-} can in undersaturated solutions react with 2H^+ to form 2HCO_3^- thus increasing the pH by consuming $[\text{H}^+]$ (Ilyina et al. 2013).

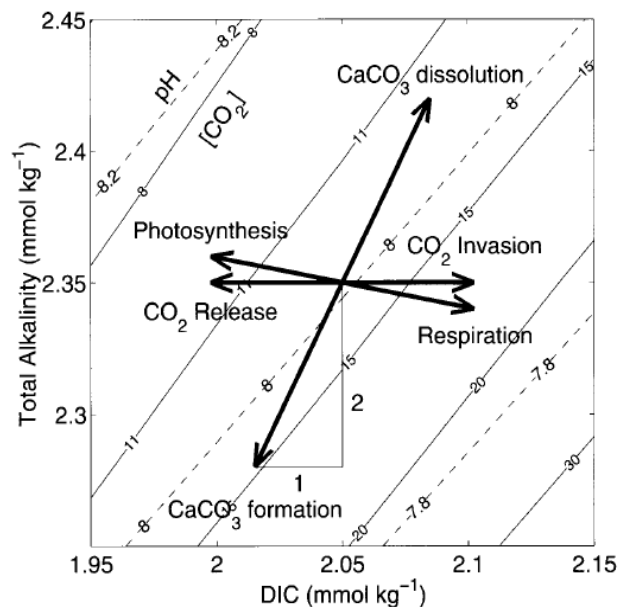
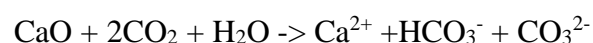


Figure 4 Overview of changes to total alkalinity and dissolved inorganic carbon: Different processes and how they affect TA and amount of DIC. Solid lines represent amount of dissolved CO₂ in $\mu\text{mol kg}^{-1}$, while dashed lines represent pH (Zeebe & Wolf-Gladrow 2001).

The ocean can however be several times supersaturated before spontaneous abiotic formation of CaCO₃ occur (Zeebe & Wolf-Gladrow 2001). Calcite and Aragonite, both are CaCO₃, share the same chemical composition, but has different crystal structure and chemical properties, like solubility. Surface water tend to be around 4 times supersaturated with aragonite while it is 6 times supersaturated with calcite. The properties of solid CaCO₃ is also an unusual as solubility increase as the temperature decrease. This is not a dominant force as more importantly for ocean distribution of CaCO₃ is how the solubility increase with pressure (Zeebe & Wolf-Gladrow 2001).

1.6 Artificial ocean alkalisation

These alterations mention is all natural but can be mimicked by artificial ocean alkalinity, AOA, technologies and accelerated processes that would otherwise remove CO₂ on a time scale of tens to hundreds of thousands of years. Disposal of CaCO₃ or olivine ((Mg, Fe)₂SiO₄ Mg:Fe ratio >90% in typical natural composition) called enhanced weathering, is proposed to artificial increase alkalinity in the ocean (Köhler, Hartmann & Wolf-Gladrow 2010). The ocean would then storage more CO₂ without increasing acidification (Baird & Cann 2012). CaCO₃ is one of the most common minerals in the earth's crust and addition into undersaturated ocean waters, regarding CaCO₃ formation, would increase alkalinity. As previously mention, however, the ocean is already saturated, and it will not lead to addition of alkalinity in most ocean waters (Ilyina et al. 2013). Such undersaturated conditions is mostly found in deep ocean, where dissolution of CaCO₃ will not cause more CO₂ uptake from the atmosphere, except when the deep water reaches the air-sea interference like upwelling zones (Feng et al. 2017). CaCO₃ disposed must therefore be dissolved in an undersaturated solution prior to the addition in surface waters if we are to expect alkalinity changes (Ilyina et al. 2013). A way to avoid this problem is by using the production formed from heating CaCO₃ (Kheshgi 1995). Utilization of CaO powder was introduced by Haroon Kheshgi as a mean of AOA, or ocean liming (OL). CaO also called quicklime would dissolve in the mixed layer, increase alkalinity and thereby sequester CO₂ in the water. The highly alkaline surface water would then eventually mix with deep ocean carrying with it the additional dissolved carbon as well (Kheshgi 1995).



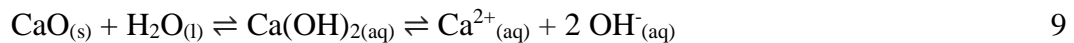
7

CO₂ diffusion in seawater without CaO (equation 8) will in contrast keep alkalinity constant but raise the seawater acidity.

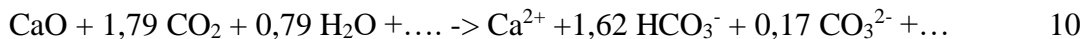


1.7 Lime cycle

Like CO₂ in the carbonic cycle, CaO is part of a natural cycle called lime cycle. In aquatic systems Ca forms oxide as CaO, and slaked lime, Ca(OH)₂. Along with the carbonic cycle the formation of limestone, CaCO₃, will appear, that can be turned back to CaO by applying energy (Schweitzer & Pesterfield 2010). The reaction between CaO and water is highly exothermic forming Ca(OH)₂ in matter of seconds (appendix F). Ca(OH)₂ will further dissolve into Ca²⁺ and 2 OH⁻ while the newly formed Ca²⁺ can react with CO₃²⁻ to form CaCO₃ depending on the saturation.



Addition of CaO and then the formation of 2OH⁻, will in undersaturated conditions therefore help increase the alkalinity. The addition of 1 mol quicklime has then the ability to add 2 mol alkalinity while not increasing the amount of dissolved organic carbon and effectively increasing and maintaining pH (Ilyina et al. 2013). However, this theoretically 2:1 ability will not be reached since a fraction of the hydroxyl and bicarbonate ions will react and form water and carbonate. The correct mol relation would instead be between 1.6 and 1.8 (Renforth, Jenkins & Kruger 2013; Kheshgi 1995).

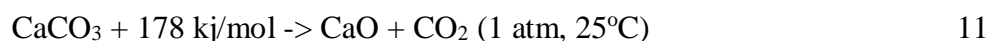


The increase of alkalinity by the dissolution of lime will end up increasing pH, then shift the carbonate systems equilibrium reducing the amount of dissolved CO₂ pressure by storing it as HCO₃⁻. This leads to a net transport of CO₂ from the atmosphere to the ocean.

There are nevertheless still many uncertainties how the ocean and organisms living there will react to a large-scale ocean liming operation. Especially to biological response to higher concentration of HCO₃⁻ and CO₃²⁻, as we know through acidification research, that organisms may be vulnerable to alteration in living conditions. Procedures for addition must be well thought through since CaO powder can lead to optic stress and even settle directly

onto organisms (Feng, Koeve, Keller & Oschlies 2016). Increased temperature from the exothermic reaction between CaO and H₂O is also a potential worry. Dissolving CaO to CaOH before addition is however a procedure to minimize this increased temperature. Ocean liming, depending on scale, would increase already oversaturated CaCO₃ conditions in the ocean. This can lead to spontaneous abiotic precipitation of CaCO₃, and make a negative feedback to the intentional alkalisation (Feng et al. 2016). The extra Ca²⁺, to an already high [Ca] (in natural ocean), will have little impact on the saturation, but via changes in the total alkalinity it will result in small changes in the decrease of total carbon by the formation of CaCO₃ (Ilyina et al 2013).

Calcium in quicklime, CaO is not the only earth alkali or alkali metal that can be used. Alkali metals in group one in the periodic table has a stronger basicity than the alkaline earth metals and Li₂O for instance is usually used in special occasion like spaceships and submarine to control CO₂ concentration. But Li₂O is more expensive than the other oxides, and alkali metals are generally more soluble than alkaline earth metals. (Wang, Yan, Ma & Gong 2011; Bobicki, Liu, Xu & Zeng 2012). The reactions between MgO or CaO with H₂O are both exothermic reactions and occur spontaneously in nature. They are therefore the ideal source for mineral carbonation (Bobicki et al. 2012). However, CaO are often the preferred alternative due to their low cost, relatively high availability from natural minerals, easy to produce and high solubility in seawater (Alvarez & Abanades 2005; Renforth & Kruger 2013; Paquay & Zeebe 2013). The solid calcium oxide, CaCO₃ formed is also easily transported and can be utilized for economically benefits. Thus, CaO is unlikely the limiting factor in ocean geoengineering (Schweitzer & Pesterfield 2010). A problem however could be the energy requirement and operational availability needed to produce CaO. To produce CaO it is usual to reverse the reaction by heating CaCO₃ to around 1000 °C and in the process producing CaO and CO₂, as seen in equation 11 (Paquay & Zeebe 2013).



To achieve a production that could make a significant difference to the atmospheric CO₂ it must reach a number of a million tons per day (Renforth et al. 2013). During 2007 around 283 million tons CaO was produced globally and is foremost used in steelmaking processes, in the construction of concrete, paper production, agriculture and used for the treatment of drinking water to name a few (Valverde, Sanchez-Jimenez & Pérez-Maqueda 2015; Miller 2007). Production should therefor increase drastically from the 2007 level to

obtain a CO₂ sequester potential on a global scale. Additional obstacles occur in the transportations and applications in the ocean. A solution could be to use the network of the worlds shipping traffic already operating. Even though they are already operating in enough regions, it would need upgrades on ships and infrastructure and increase fuel consumptions, again adding to the world's total emission (Paquay & Zeebe 2013; Renforth et al. 2013). Shore based application close to present infrastructure could limit energy demand in transportation, but also limit global potential as effect would be more regional. Protection of especially fragile ecosystems in keeping the saturation states and pCO₂ close to present-day values are also a possible application to “buy some time”. This must be a long-term investment as an abruptly end of application in a business-as-usual scenario would lead to a more rapid shift to acidified conditions that we experience today (Feng et al. 2016)

1.8 Complementary research

The formation of CO₂ and CaO from CaCO₃ is a highly endothermic reaction (equation 11) that would additionally increase the global energy usage (Paquay & Zeebe 2013). Without consideration, this would cause a direct or indirectly effect on total CO₂ emission (Paquay & Zeebe 2013). From production of a ton pure CaCO₃ it would generate around 440 kg highly pure CO₂ gas (with additional purification reach CO₂ >98 %) when fully calcinated (Renforth et al. 2013). All or almost all the CO₂ produced in the reaction should therefore be captured and stored to stop adding to the problem. CO₂ from quicklime production may though be easier to capture than other more “contaminated” sources as highly pure CO₂ gas can be captured directly from the industrial source for geological storage (Manahan 2017).

Carbon capture and storage (CCS) has been considered as a practical option to limit the CO₂ concentration, and will probably increase in importance if ocean liming would be operational (Wang et al. 2011). CaO has in addition to ocean liming been investigated has a component in CCS (Valverde et al. 2015; Grasa, Martínez, Diego & Abanades 2014). Multi-cycling calcination/carbonation of limestone called Ca-looping technology, is based on the quick reaction between CaO and CO₂ which is cycled several times for capture and release of CO₂. A problem this technology is facing is the effectiveness for CaO to “carry” CO₂ decrease with number of calcination/carbonation cycles (Grasa et al. 2014).

Geological reservoirs, ocean sequestration and utilization into industries are all useable technologies that offers different possibilities. Geological reservoirs like depleted mines, oil and gas fields are optional solution with huge storage potential, but the chance of a bulk leakage will always be a devastating risk. While industrial usage of CO₂ in building material might have limiting capacity and storage time (Bobicki et al. 2012). Sequestrations of CO₂ gas directly into the water would acidify nearby waters and be time-limited as it will rise back towards the atmosphere.

To be able to keep CO₂ in the ocean for a substantial amount of time it should be liquified, which begins at pressure higher than 5.1 bar (Baird & Cann 2012). Liquid CO₂ is much more compressible than liquid water and at pressure over 127 bar the density of CO₂ will be higher than for water. The exact depth will depend on water temperature, but by assuming 1 bar for 10 m water, depth needs to be more than 2700 m. However, since the ocean temperatures are less than 9 °C the liquid or packed gas would form hydrates with water and solidify and sink (Baird & Cann. 2012). The average depth of the ocean is 3800 m so there is a substantial capacity for sequestration, but costs are high, and earthquake is still a risk. A liquid lake of CO₂ would also exterminate the habitat for any present organisms. Sequestration of CO₂ direct into the ocean leads to acidification, with pH decreasing several units close the injection point.

1.9 Ionic strength and activity

In more saline water like seawater, contrary to fresh water it is important to consider the ionic strength. More and different ions in a solution will increase how much they interact with each other with long-range electrostatic interactions, ion-pairing and complex formations causing them to chemically behave like they are less-concentrated than what they can be measured (Zeebe & Wolf-Gladrow 2001). Ionic strength is based on the charge and concentration of the dissolved ions in the solution and higher the charge the weaker the activity and vice versa (Stumm & Morgan 1996). In seawater NaCl is the major component, but properties for seawater and pure NaCl differ as the seawater mixture include other ions with different charge that must be considered. The salinity of the solution can be calculated and show a linear relationship with the ionic strength, equation 13 (Zeebe & Wolf-Gladrow 2001).

$$I = 1/2 \sum \text{concentration} \times \text{charge}^2$$

12

$$I = 1/2 ([Cl^-] \times 1 + [Na^+] \times 1 + [Mg^{2+}] \times 4 + [SO_4^{2-}] \times 4 + \dots) \sim 0,7 \quad 13$$

The degree in which the constituent's effective concentration and the real concentration, [C] are compared are termed activity, {A} and an activity coefficient, μ_a is needed for the species in question.

$$\{A\} = \mu_a \times [C] \quad 14$$

In infinite dilute solution the concentration of competing ions is ignored, and we can say activity is equal to the relevant concentration (Zeebe & Wolf-Gladrow 2001).

$$\text{Ideal solution: } \{A\} = 1 \times [C] \quad 15$$

In seawater the situation is complicated and the conversion from concentrations to activities at around seawater salinity require uncertain calculations of the activity coefficient (Zeebe & Wolf-Gladrow 2001).

1.10 Finding pH

In the original definition for determination of pH introduced by Sørensen (1909), pH is the negative logarithm of the H^+ concentration, but in aqueous solution the amount of “free hydrogen” does not exist in a significant amount (Zeebe & Wolf-Gladrow 2001). The hydrogen is instead bound with water in the form of H_3O^+ which is bound to more water molecules forming $H_9O_4^+$, thus the free hydrogen represents more the hydrate complex. It is also noticeable that the effective concentration of free hydrogen is affected by surrounding ions and an activity coefficient is needed (Stumm & Morgan 1996).

$$pH = - \log [H^+] \quad 16$$

$$pH_{\text{activity}} = - \log \{H^+\} = - \log [H^+] \times - \log \mu_{H^+} \quad 17$$

$$[H^+] = \{H^+\} / \mu_{H^+} \quad 18$$

In seawater there are many constituents, but some notable major ions like SO_4^{2-} and F^- binds with free hydrogen ions. Along with water complexes, these reactions must be accounted for to get an accurate pH reading (Zeebe & Wolf-Gladrow 2001).



In measuring pH, it is important to consider which pH scale to use as different scales can differ up to 0.12 units. Because of the, in comparison, big contribution of HSO_4^- the difference between the total scale and seawater scale are small and only differ about 0.01 (Zeebe & Wolf-Gladrow 2001).

1.11 Kinetics

Most reactions in the ocean are described as in chemical equilibrium that strives toward a steady state situation. Reactions will still take place all the time, but the forward and backward reactions happen simultaneously, and the rate of the reaction are equal (Zeebe & Wolf-Gladrow 2001). Instead of chemical equilibrium, chemical kinetics are more of an interest when reactive elements are introduced. Chemical kinetics helps describe reactions that are one way driven towards equilibrium where the concentrations of the reactants change during time (Zeebe & Wolf-Gladrow 2001).

$$\text{Rate} = d\xi/Vdt \quad 21$$

$$\xi = (n_i - n_{i0})/\nu_i \quad 22$$

The rate of a chemical reaction can be expressed as equation 21, where ξ denote the extend of the reaction defined by the relevant substance change of the number of moles divided by its stoichiometric coefficient(ν), n_i is the number of moles present at a specific time, n_{i0} the initial number of moles, V is the volume, and the t is time (Brezonik 2018).

$$\text{Rate} = dn_i / \nu_i V dt = d[C_i] / \nu_i dt \quad 23$$

With differentiating equation 22 in respect to time and substituted it into equation 21 you get equation 23 thus showing the reaction rate is equal to the change in concentration of a reacting species divided by its stoichiometric coefficient (Brezonik 2018). Finding the rate of the reaction will determine which reactant controlling the speed and needed to predict the destiny between CaO and seawater. It is important to note that in a kinetic perspective concentration is used instead of activity as the reaction is dependent on the number of colliding molecules per volume (Zeebe & Wolf-Gladrow 2001).

Table 2 Reaction order: k is the rate coefficient or rate constant and its measurement unit depend on the order of the reaction. The most common way to evaluate rate constants is by graphically plot a function based on the rate equation and reaction order. (Brezonik 2018; Zeebe & Wolf-Gladrow 2001).

| Order | Rate equation |
|--------|----------------------|
| Zero | $-d[A]/dt = k$ |
| First | $-d[A]/dt = k[A]$ |
| Second | $-d[A]/dt = k[A][B]$ |

The reaction order can be determined by data produced which can be integrated into one of the rate equations (Brezonik 2018). Some reactions rates are not depended on the concentration of the reactant. These reactions are called zero order reactions and the rate constant will be equal to rate of the reaction. If the reaction rate is influenced only of the concentration of a single reactant, A it is a first order reaction. Second order reaction is influenced by two reactants, A and B or 2A. Although the total reaction is second order the reaction can still be first order for each of the reactants, A and B ($1+1=2$) (Zeebe & Wolf-Gladrow 2001). Reaction can also be third order when three reactants are deciding the rate, but this is less common except when catalysis is involved (Brezonik 2018).

Many reactions include several steps and intermediates before the final product appear. In these reactions it is the slowest step that decide the overall reaction rate, but if some of the steps are comparable in magnitude, they both must be included (Brezonik 2018).

Temperature is a factor that could alter the reaction rate. Since the energy of the molecules increase with temperature, there are more molecules reacting with enough energy to overcome the activation energy so the rate-constant increase (Zeebe & Wolf-Gladrow 2001). Present ions in a solutions can also alter the reaction kinetics by ion interaction or forming complexes with the reactive ion (Morse & Mackenzie 1990). Nearby opposite charged ions will reduce the electrostatic attraction and therefore reduce the reaction rate while same charged ions reduce the electrostatic repulsion and increase the reaction rate (Zeebe & Wolf-Gladrow 2001). In some cases, the data produced will not fit any of the rate expressions or fit several of them equally well, and lead to trouble selecting the order (Brezonik 2018). This can be caused by sampling mistakes, misunderstanding of reaction pathways, pH variations, ion effect and back reactions. Also, when carbonate is involved in the kinetics organic matter may not only chemically interact but act as a physical coating (Morse & Mackenzie 1990).

1.12 Scope and calculation

In engineering the natural storage of carbon by using the largest reservoir of CO₂, a contribution to reversing global warming and acidification could be possible. Geoengineering can lead to unknown problems, but also solutions. This thesis will use one the most common used oxides, calcium oxide and explore its effect on alkalinity, pH and the transformation of inorganic carbon species in the carbonic cycle. Additional experiment will try to determine chemical kinetics using different concentration of CaO and asses the possibilities for XRF as a tool for in-situ PIC determination. To find the four carbonate system parameter, Σ dissolved inorganic carbon, total alkalinity, pH and partial pressure of CO₂, only pH and alkalinity will be measured as the other can be calculated based on those data produced (Zeebe & Wolf-Gladrow 2001). Since little literature can be found on this subject this study, as a preliminary experiment, will hopefully bring some light on the possible problems or possibilities.

2. MATERIAL AND METHOD

2.1 CaO

Since CaO is expected to react with water and CO₂, procedures had to be in place to limit humidity and exposure from air and respiration. All glass material, magnets, spatulas and petri dish were therefore washed with milli-Q water and then placed in a heating chamber at 60 °C for at least one hour before contact with CaO powder or extracted samples. Plastic material used include spatulas, petri dishes, containers and vials, and are all made of polyethylene.

Two types (coarse and fine) of fresh CaO was delivered by Miljøkalk AS for usage in this experiment. In an attempt to limit humidity and lower the temperature the two glass bottles were packed in bubble wrap and stored in a fridge. A plastic spatula was used for underlayer for weight measurement and transportation to the experimental setup. Before every extraction the bottles were turned to get unexposed CaO to the surface and extracted using a metal spatula. Exposure time to fresh air was approximately 10 minutes for each trial and from delivery of product to end of experiments was around 1 ½ months. The mineral was in powder and grain-form and had a white or slightly beige colour. The fine CaO diameter is between 0.2-0.8 mm with a specific surface area of 1.53 m² g⁻¹ and is expected to contain 94% active CaO. While the coarse CaO has a diameter between 0.5-2.5 mm with a specific surface area of 1.12 m² g⁻¹ and is expected to contain 91 % active CaO (More CaO specs can be obtained from appendix F).

2.2 Seawater

Seawater used in this experiment have been collected at Trondheim's Biological Station, TBS seawater that is pumped up from 100 m depth in Trondheimsfjorden. The water was collected in late autumn, 2018 and during the experiment seawater was collected multiplied times in four HDPE containers. The water was not fine-filtered and storage time was between hours and up to one week before being utilized. Trondheimsfjorden is an enclosed estuary with salinity alteration expected to be between 30-35. Salinity was not determined in this experiment, but for calculation the salinity was set as 33,6 from TBS

measurements in winter 2018. Particular organic carbon, POC content is expected to be approximately $40 \mu\text{g C L}^{-1}$ (M. V. Ardelan, personal communication, May 4, 2019).

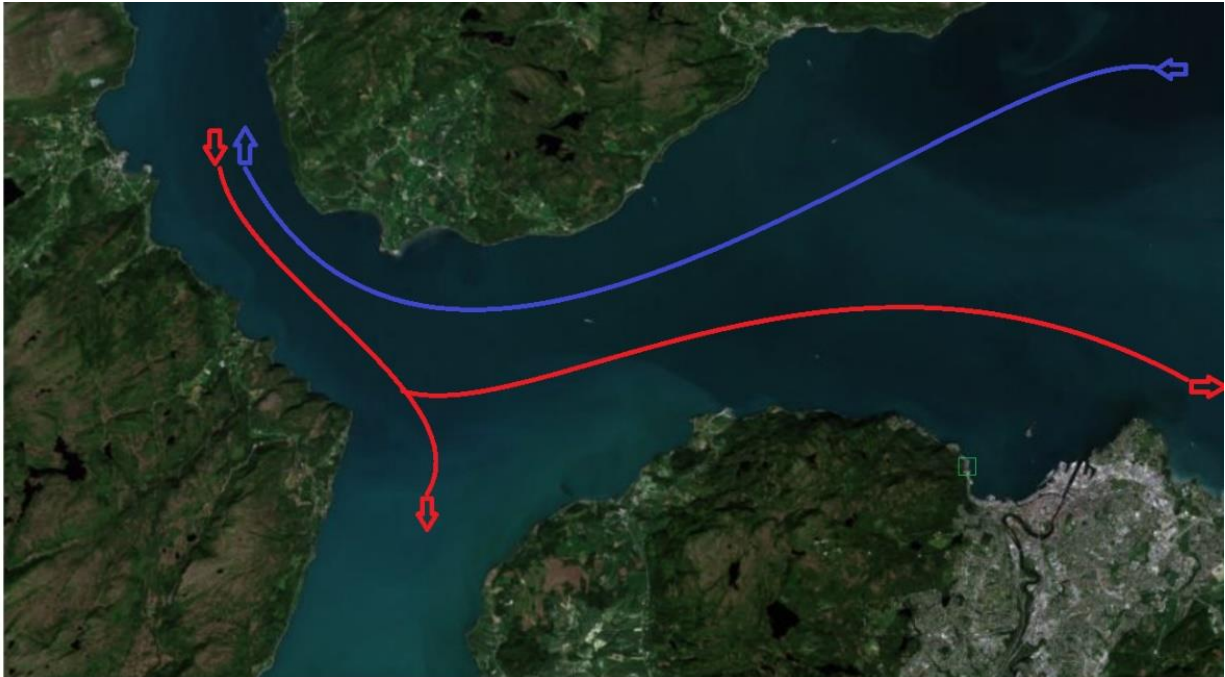


Figure 5 Overview of Trondheimsfjorden inlet and TBS: Part of Trondheimsfjorden with a simplified current overview where red arrows represent current going into the fjord from the ocean while the blue one is going outward according to the Coriolis effect. Which current dominates are in main decided by the tide. The green square shows TBS's location. Map is retrieved from the Norwegian Mapping Authority ("Trondheimsfjorden")

2.3 pH calibration

Two different kinds of pH electrodes were used; *Orion™ 8102BNUWP ROSS Ultra™ pH Electrode* (A) and *WTW™ SenTix™ 81 pH Electrode* (B) with KCl electrolyte that was connected to *Orion™ Dual Star™ pH, ISE, mV, ORP and Temperature Dual Channel Benchtop Meter*. Calibration was conducted as described by the manufacturer own manual. The electrode was rinsed in milli-Q water and dried with kimwipes in between using the three buffers. The same procedure was applied every time the pH electrode was used in samples. At $14 \text{ }^\circ\text{C}$ the three NBS buffers had a pH at 4.01 ± 0.02 , 7.02 ± 0.02 and 10.05 ± 0.05 . The beaker containing the buffer and the electrode was hold in upper part with gloves to limit heat transfer and gently shaken until the pH meter had received a stable reading. The calibration was for this experiment acceptable when the average slope was over 96 %.

2.4 Test to find right dose of CaO

Desired alteration of pH in this thesis was around 0.5, so to find the right amount of CaO to be used a preliminary experiment was designed. Fine CaO was expected to react faster than coarse and therefore chosen to be added to a full 10 L container in dosages of 0.05 g. Before and after each addition of CaO and before extraction of samples the container was manually turned and shaken between 30 to 60 seconds. Sampling intervals was every 5-10 minute and lasted for 90 minutes. Addition of doses happened as pH seemed to be stable from the previous addition, approximately every 20 minutes. Additional pH-readings took place after 14 hours and 45 minutes, 18 hours and 30 minutes and 5 days. pH was monitored by putting the pH electrode (B) in a vial with 30-50 mL extracted sample. Temperature was measured with a glass mercury-thermometer in the beaker as it was gently shaken. The beaker was hold in the upperpart to not transfer heat. In total 5 doses of ~0.05 g CaO were used in this test.

2.5 Alkalinity and pH

For the rest of the experiments it was decided to use a laboratory with temperature control to be able to lower the experimental temperature. The temperature in the laboratory was ~14 °C which was also used as storage for the seawater. Seawater usage per trial also increased to 15 L. The container was before and during each trial placed on a VWR® *Standard Orbital Shake* with in the intention of mixing the contain more homogenous. Amount of 0.15 g CaO (or ~0.01 g L⁻¹) derived from the preliminary test, stayed constant during measurement with different grains. Additional pH measurement was concluded with 0.225 g and 0.3 g CaO in the same 15 L tank.

Alkalinity is in this study measured by titrating the actual seawater sample with 0.01 M HCl in the burette. In each sampling 30 mL was extracted trough a tap of the container. The pH electrode (B) was then placed in the beaker and the solution was stirred using a magnet stirrer. Each titration took about 2 minutes and ended when pH in the beaker stabilized at 3.7 ± 0.05 . The volume 0.01 M HCl used in each titration was noted to be used for alkalinity calculation.

Four trials of pH measurement are included for consideration. Two for both fine and coarse CaO, and two with increased CaO. In the second trial the electrode (A) was placed in a

hole in the container attached with traditionally grey duct tape to get accurate pH measurement continuously. In the first ten minutes sampling happened as fast as possible, but as less changes were observed the sampling intervals decline. Alkalinity measurement took place simultaneously with this trial that lasted for 6 and 8 hours for fine and course CaO respectively. The shaking intensity during was medium/high and a stopwatch was used to control the time that was noted beside each actual measurement.

2.6 Activity coefficient and alkalinity calculation

For pH and alkalinity calculation an activity coefficient must be included. The coefficient was decided by preparing 30 mL of a series of standard solutions of HCl (0.008-0.016) and mix them separately with 100 ml actual seawater. A pH electrode (B) was used to find a_H (activity) which was plotted against the acid solutions. From the slope the f_H (activity coefficient) can be determined. For the seawater collected from TBS the f_H is set as 0.77 for pH and alkalinity calculations (M. V. Ardelan, personal communication, May 3, 2019).

$$a_H = 10^{-pH} \quad 24$$

$$A_t = \left(\frac{1000}{V_s} * V_a * C_a \right) - \left(\frac{1000}{V_s} * (V_s + V_a) \right) * \frac{a_H}{f_H} \quad 25$$

Total alkalinity (A_t) is calculated as seen in equation 25 where V_s is the sample volume (30 mL), V_a the volume added titrant (ranged from 7.9 to 8.8 mL) and C_a the concentration of the titrant (0.01 M HCl). The solution was titrated to pH 3.7 which is used to calculate a_H seen in equation 24.

2.7 Filtrations

The main focus in this thesis include four trials including of one 0.15 g experiment for both coarse and fine CaO, one 0.225 g and one 0.3 g fine CaO. As for alkalinity and pH measurement temperature stayed at ~14 °C, a 15 L container was used for seawater and the shaker was set on medium/high intensity. Around 1 minute of manually shaking and turning of the container was performed before and after the addition of CaO and samplings for filtrations. Sampling intervals for coarse CaO was every 15 minutes and lasted for 5 hours while it was every 10 minutes for fine CaO and continued for 3 hours and 20 minutes. The

average time for the filtrations was approximately 2 minutes and both the glass beaker and the funnel was rinsed with milli-Q water to be sure all material went through the filters. A sampling included two replicas of 200 mL seawater vacuum filtrated using glass fibres filter, GFF that retain fine particles down 0.7 μm . Before filtration the GFF had to be prepared by being baked in a furnace for 6 hours at 450 °C. From the furnace to application the GFF was stored in aluminium foil and only handled by metal tweezers that was rinsed in between with methanol. Completed filters from a filtration was then put into a petri dish and stored in a desiccator.

Along with the solid material gathered by the filter papers it was necessary to analyse the liquid phase in the same four trials. The water was pressed trough a *Sartobran® Capsule 0.2 μm* filter with a syringe in two replicas in the same intervals as the vacuum filtration. 4- 6 mL seawater was pressed trough and additionally repressed with air additional four times using the same syringe. The filtrate was extracted into sealed 15 mL metal free centrifuge tubes. The syringe and 0.2 μm filter were rinsed with pressing milli-Q water trough between sampling.

Additional vacuum filtration trial of 0.15 g fine CaO was necessary for XRF. Same conditions for sampling was applied. Two replicas with interval starting at every 10 minutes but was extended during the experiment. Unlike previous trials they were dried in a furnace at 60 °C in 30 minutes before being stored in a desiccator.

2.8 Preparation, analysing and DIC calculation

The filtrate was analysed for the isotopes ^{25}Mg , ^{44}Ca , ^{56}Fe , ^{60}Ni , ^{63}Cu and ^{88}Sr by inductively coupled plasma mass spectrometry, ICP-MS. To prevent ions to adhere to the tube wall and by then overlooked, two drops of 0.1 M HNO_3 was added to every tube before readings. Relevant data from in total 160 samples from four trial with two replicas each plus three blanks was gathered.

For total particular carbon (PIC + POC) determination 167 filters were packed into tinfoil caps for non-dispersive infrared absorption. Even though the particular analysing technic is usually used for POC it can be applied for this purpose as the expectation for organic development are low. PIC is then decided by subtracting the total particular carbon with 40 $\mu\text{g C L}^{-1}$ which is the expected POC level. The technic is based on burning the sample

measuring the amount of CO₂ and NO_x gases being exposed. The still humid samples were folded with methanol washed tweezers and placed in a HDPE plastic matrix covered with aluminium foil in awaiting burning.

In the setup for XRF analysing it was important to remove any exposure to other elements, especially heavier (meaning elements with atomic number 11 or higher in the periodic table) beside those that could be found in the filter. As the radiation focused on low concentration of heavy elements and mostly lighter (C, N, H, O) the exposed area will increase so precautions preparations as operational direction planning along with metal barrier was put up. The handheld instrument, NITON XRF Analyzer was placed in stand placed downward approximately 50 cm from the floor. The filters were transferred on top of a petri dish upon a plastic container around half a centimetre from the radiation source, so the focused beam covered the entire filter. The instrument was set with standardized mining setup that covered main, low and light range elements without helium gas. Every fifth second it switched between the different ranges and lasted for 65 seconds. In all 42 datasets from two repetitions (trial A and B) of the 20 samples with two replicas and two blanks was gathered.

Calculations of DIC species was follow through with CO2SYS EXCEL Macro spreadsheet version 2.1 (18.09.2012) created by Dr. D. Pierrot using code developed by Ernie Drs. Lewis and Doug Wallace. In the calculation the carbonate dissociation constant from Mehrback et al (1973) refit by Dickson and Millero (1987), the dissociation constant for KHSO₄⁻ is from Dickson (1990), the total boron formulation from Uppstrom (1974) and the pH scale used is the NBS scale. For all calculations the temperature is set as 14 °C and the salinity as 33.6.

3. RESULTS

3.1 Test result to find right dose CaO for main experiment

The reaction between CaO and H₂O is exothermic (section 1.7), but any obvious temperature changes was not observed at this level of dosage and basic equipment.

As the CaO particles dissolved the liquid stayed clear but some amount of white precipitate was observed after several additions. In this first probing experiment CaO addition lead to incline in pH values in matter of minutes, and as more dosed was added the higher the imminent alteration occurred, figure 1. Late pH readings after 14 hours, 18 hours and 5 days had pH values of 9.1, 8.9 and 8.9 accordantly. The amount of precipitate after 5 days seemed to have increased, but not drastically.

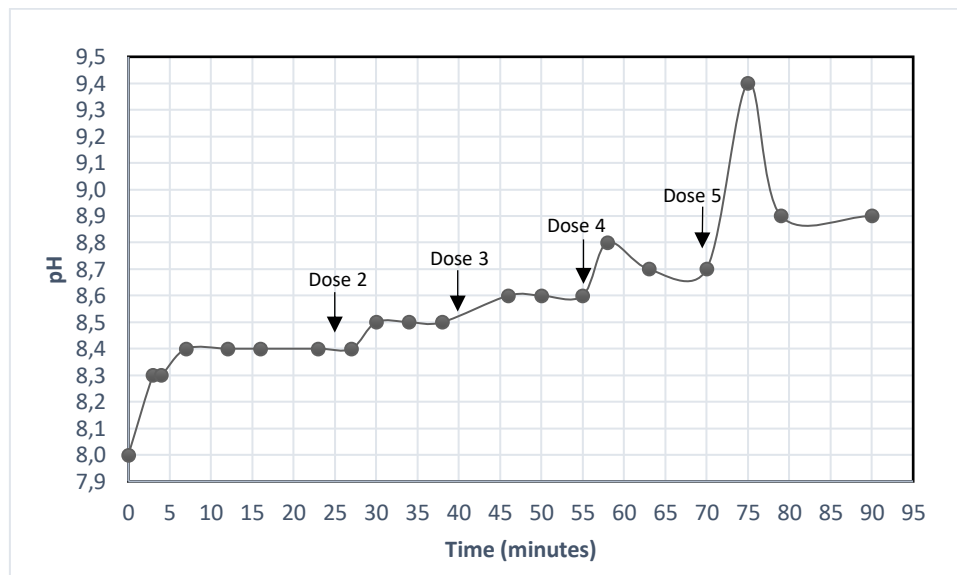


Figure 6 pH changes from increasing amount of CaO: pH alteration after addition of fine CaO in seawater at 20 °C, 1 atm. The average slope for the pH meter(A) was found to be 96.5 %. Additions of doses happened as follow; Dose 1 after 0 minutes: 0.0583 g, Dose 2 after 25 minutes: 0.0482 g, Dose 3 after 40 minutes: 0.0562 g, Dose 4 after 55 minutes: 0.0552 g, Dose 5 after 1 hour and 10 minutes: 0.0560.

3.2 Results from fine and coarse grained CaO

3.2.1 pH, alkalinity for fine grained CaO

Measurement of pH in this part were done continuously in the container as the reaction went on. First attempt to measure pH by taking out samples externally was problematic as the rapid changes seen in figure 7 and figure 8 was hard to pinpoint for a specific time. Uncertainty about how reliable they were led to not include them (appendix A).

The powdery CaO, $\sim 0.01 \text{ g L}^{-1}$ CaO seawater, were visible immediately after addition, but when shaking began it disappeared. The pH of the solution changed from 7,84 to 8,25 in the first 10 minutes of the reaction. The rate of change then declines up to one hour where it stagnated with only minor changes, 0,02 (8,50 at 60 minutes and 8,53 at 360 minutes). The highest pH value was measured 8,53 after 245 and 250 minutes.

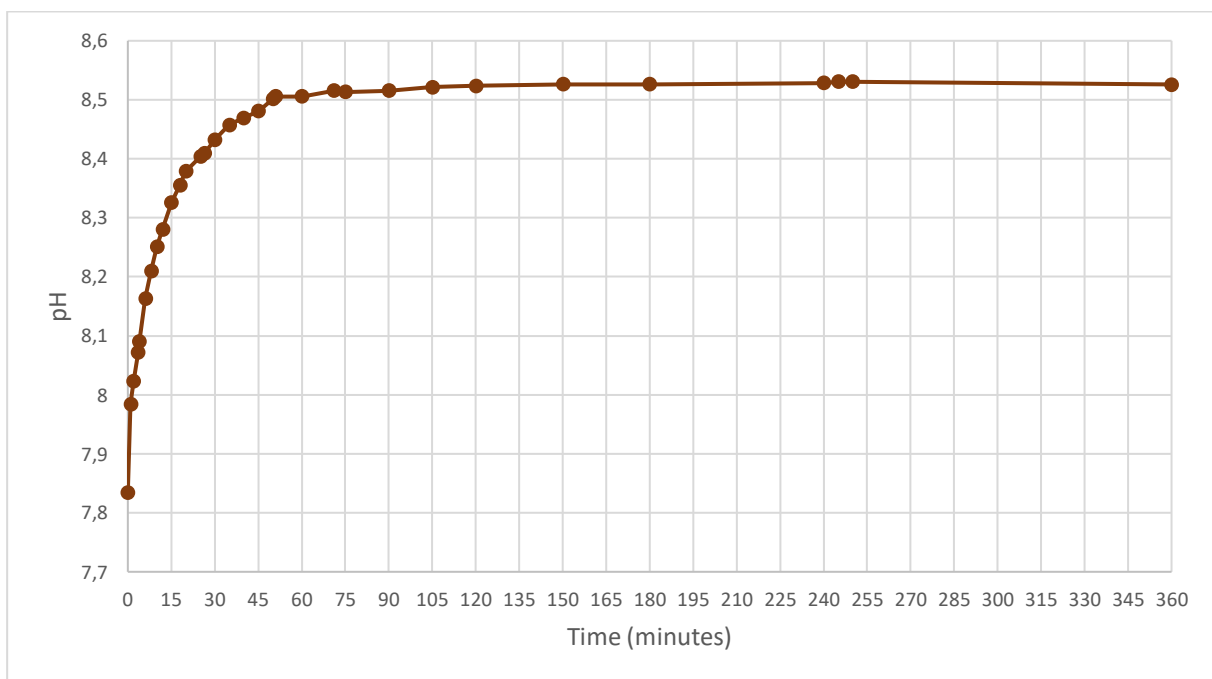


Figure 7 pH values after $\sim 0,01 \text{ g L}^{-1}$ fine CaO mixed in seawater: 0.1508 g fine CaO was mixed with 15 L seawater at 14°C , 1 atm. Changes in pH was monitored as the reaction went on. The average slope for the pH meter(A) was found to be 96.3 %. Salinity is expected to be 33.6. Dataset is presented in appendix A.

Like external measurement of pH, it was problematic to pinpoint a precise time for the external alkalinity measurement. For each sampling it took between 2 to 3 minutes for seawater to be extracted from the tank and titration finalised. Two scheduled samplings after

40 and 45 minutes went wrong leaving an unplanned gap in the dataset, presented in table 3 and appendix B.

Changes in TA of seawater increase as CaO react and increase from 2363.6 $\mu\text{Eq L}^{-1}$ to a stagnating point after 90 minutes, 2663.2 $\mu\text{Eq L}^{-1}$. The value after 90 minutes are same values measured after 360 minutes, which conclude the measurement. A deviating single maximum value was found after 245 minutes when TA = 2679.8 $\mu\text{Eq L}^{-1}$.

From pH and alkalinity measurement taken simultaneously (appendix A and B) Total DIC (TCO_2), $[\text{HCO}_3^-]$, $[\text{CO}_3^{2-}]$, $[\text{B}(\text{OH})_4^-]$ and $[\text{OH}^-]$ values in table 3 was calculated using CO2SYS EXCEL Macro spreadsheet.

A change of carbon species appears after CaO addition. $[\text{HCO}_3^-]$ decrease 298.4 $\mu\text{mol kg}^{-1}$ -seawater while $[\text{CO}_3^{2-}]$ increase 251.1 $\mu\text{mol kg}^{-1}$ -seawater along with $[\text{B}(\text{OH})_4^-]$ 91.5 $\mu\text{mol kg}^{-1}$ -seawater and $[\text{OH}^-]$ 4.2 $\mu\text{mol kg}^{-1}$ -seawater. Total DIC alterations, although changes in both directions decrease from start to endpoint with 76.4 $\mu\text{mol kg}^{-1}$ -seawater.

Table 3 Changes in alkalinity species after $\sim 0.01 \text{ g L}^{-1}$ fine CaO addition: 0.1508 fine CaO was mixed with 15 L seawater at 14°C, 1 atm. Salinity is expected to be approximately 33.6. Alkalinity measurement from titrating sample with 0.01 M HCl and calculated with CO2SYS EXCEL Macro spreadsheet.

| Time | Total alkalinity | DIC | HCO_3^- | CO_3^{2-} | B alk | OH^- |
|------|------------------|---------|------------------|--------------------|--------|---------------|
| 0 | 2363,62 | 2279,32 | 2161,43 | 82,32 | 36,41 | 1,15 |
| 3,5 | 2396,90 | 2228,25 | 2076,89 | 130,67 | 56,77 | 1,90 |
| 12 | 2513,39 | 2233,10 | 2015,50 | 205,19 | 84,44 | 3,07 |
| 18 | 2546,67 | 2218,37 | 1969,83 | 238,34 | 96,51 | 3,65 |
| 26,5 | 2563,31 | 2198,25 | 1925,61 | 263,84 | 105,90 | 4,14 |
| 51 | 2613,23 | 2174,50 | 1851,31 | 316,41 | 123,96 | 5,16 |
| 60 | 2629,87 | 2189,07 | 1863,71 | 318,53 | 123,96 | 5,16 |
| 71 | 2629,87 | 2181,54 | 1851,16 | 323,75 | 125,93 | 5,28 |
| 90 | 2663,15 | 2210,60 | 1875,82 | 328,06 | 125,93 | 5,28 |
| 105 | 2663,15 | 2206,01 | 1868,14 | 331,27 | 127,13 | 5,35 |
| 150 | 2663,15 | 2202,17 | 1861,72 | 333,95 | 128,12 | 5,42 |
| 245 | 2679,79 | 2213,56 | 1868,77 | 338,32 | 128,93 | 5,47 |
| 250 | 2663,15 | 2199,08 | 1856,55 | 336,11 | 128,93 | 5,47 |
| 360 | 2663,15 | 2202,94 | 1863,00 | 333,41 | 127,92 | 5,40 |

3.2.2 pH, alkalinity for coarse grained CaO

Coarse grained, compared to fine grained CaO have a smaller specific surface area, 1.12 m²/g to 1.53 m²/g and a slower reaction was expected, that lead to a longer sampling period. Unlike for fine CaO, the grains did not immediately vanish after being shaken in the tank.

Like figure 7 the rate of pH changes in regard to time in figure 8 declined as the reaction went on. Changes in pH for coarse grained are not as rapid as for fine grained CaO and stagnation in alteration occur after 455 minutes, pH 8.52. A late sampling taken place 20 hours and 40 minutes after addition shows a 0.01 increase to pH 8.53, (appendix B), which is the maximum value measured.

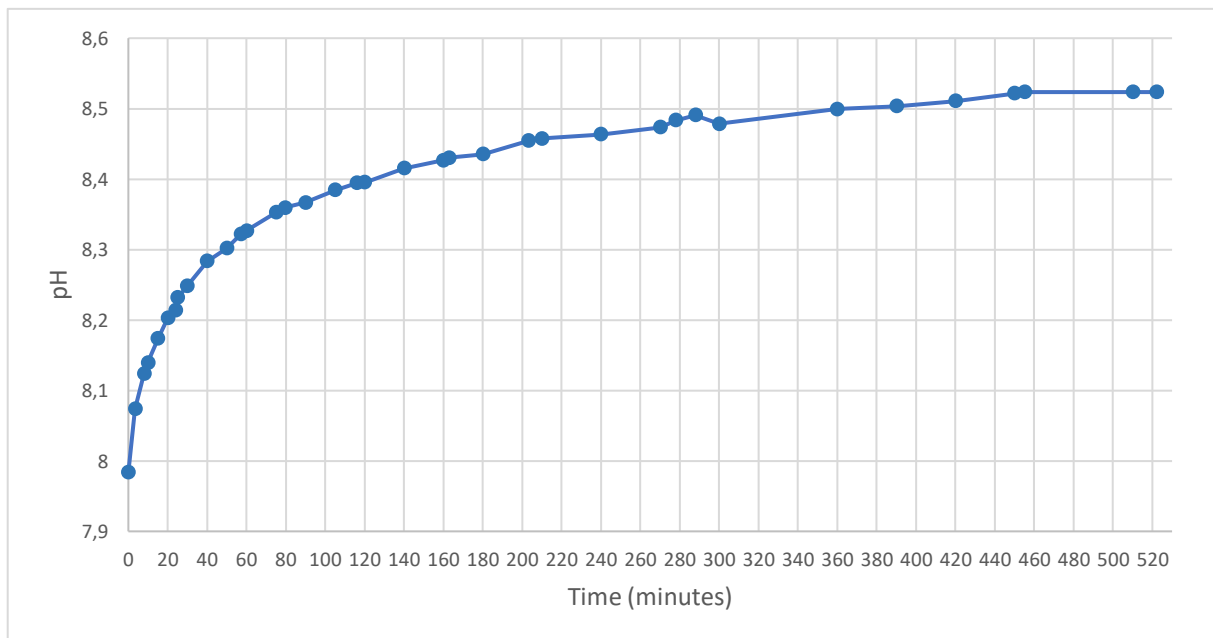


Figure 8 pH values after ~0.01 g L⁻¹ coarse CaO mixed in seawater: 0.1519 coarse CaO was mixed with 15 L seawater at 14°C, 1 atm. Changes in pH was monitored as the reaction went on. The average slope for the pH meter(A) was found to be 98.7 %. Salinity is expected to be 33.6 Dataset is presented in appendix A.

Alteration in alkalinity, table 4 was established in the third sample 15 minutes after addition and steadily increased afterwards. At 288 minutes TA = 2646.5 μEq L⁻¹ which is the same value reached after 455 and 522 minutes although it dips to 2629.9 μEq L⁻¹ in-between. In the same time range [HCO₃⁻] (246.1 μmol kg⁻¹-seawater) decrease while [CO₃²⁻] (229.9 μmol kg⁻¹-seawater), [B(OH)₄⁻] (81.9 μmol kg⁻¹-seawater) and [OH⁻] (3.9 μmol/kg-seawater) increase. Total concentration of DIC drops 58.6 μmol kg⁻¹-seawater (2232.2 to 2173.6 μmol

kg⁻¹-seawater) in the first 8 minutes but stabilize afterwards and increase up to 2196.8 μmol kg⁻¹-seawater 522 minutes after initial addition.

The seawater used for fine and coarse measurement was collected on the same date a few minutes apart. The alkalinity and pH conditions initially in the tanks was TA = 2363.6 μEq L⁻¹ with pH = 7.98 and TA 2363.6 μEq L⁻¹ with pH 7.85 respectively for the tanks designated for coarse and fine CaO. From start to end the alkalinity for coarse grained CaO changed by 283 μEq L⁻¹ while pH changed by 0.54 units. For fine grained CaO the alkalinity changed by 300 μEq L⁻¹ and pH by 0.67 units. Additional deviation appears as the rate of changes by all parameters in regard to time is faster for fine CaO than coarse. The main measured differences between coarse and fine grained CaO addition is illustrated in figure 9.

Table 4 Changes in alkalinity species after ~0.01 g L⁻¹ coarse CaO addition: 0.1519 coarse CaO was mixed with 15 L seawater at 14°C, 1 atm. Salinity is expected to be approximately 33.6. Alkalinity measurement from titrating sample with 0.01 M HCl and calculated with CO2SYS EXCEL Macro spreadsheet.

| Time | Total alkalinity | DIC | HCO ₃ ⁻ | CO ₃ ²⁻ | B alk | OH ⁻ |
|------|------------------|---------|-------------------------------|-------------------------------|--------|-----------------|
| 0 | 2363,62 | 2232,25 | 2098,82 | 107,83 | 47,60 | 1,55 |
| 3,5 | 2363,62 | 2195,68 | 2046,07 | 129,33 | 57,00 | 1,91 |
| 8 | 2363,62 | 2173,65 | 2013,09 | 142,77 | 62,86 | 2,14 |
| 15 | 2396,90 | 2181,48 | 2006,05 | 159,63 | 69,20 | 2,40 |
| 24 | 2413,54 | 2177,02 | 1989,18 | 173,56 | 74,63 | 2,63 |
| 40 | 2463,47 | 2185,45 | 1971,31 | 202,08 | 84,90 | 3,09 |
| 57,5 | 2496,75 | 2193,82 | 1963,18 | 219,65 | 90,90 | 3,38 |
| 90 | 2496,75 | 2166,24 | 1918,47 | 238,08 | 98,37 | 3,75 |
| 116 | 2530,03 | 2178,31 | 1915,67 | 253,57 | 103,23 | 4,00 |
| 163 | 2546,67 | 2169,18 | 1889,27 | 271,68 | 109,70 | 4,34 |
| 203 | 2563,31 | 2167,39 | 1874,75 | 284,91 | 114,15 | 4,59 |
| 278 | 2629,87 | 2205,39 | 1890,89 | 307,21 | 119,67 | 4,90 |
| 288 | 2646,51 | 2214,85 | 1894,81 | 312,85 | 121,02 | 4,98 |
| 360 | 2629,87 | 2193,55 | 1871,18 | 315,42 | 122,78 | 5,09 |
| 390 | 2629,87 | 2190,56 | 1866,20 | 317,49 | 123,56 | 5,14 |
| 455 | 2646,51 | 2189,98 | 1853,31 | 330,15 | 127,52 | 5,38 |
| 522 | 2646,51 | 2189,98 | 1853,31 | 330,15 | 127,52 | 5,38 |
| 1240 | 2663,15 | 2196,76 | 1852,67 | 337,73 | 129,53 | 5,50 |

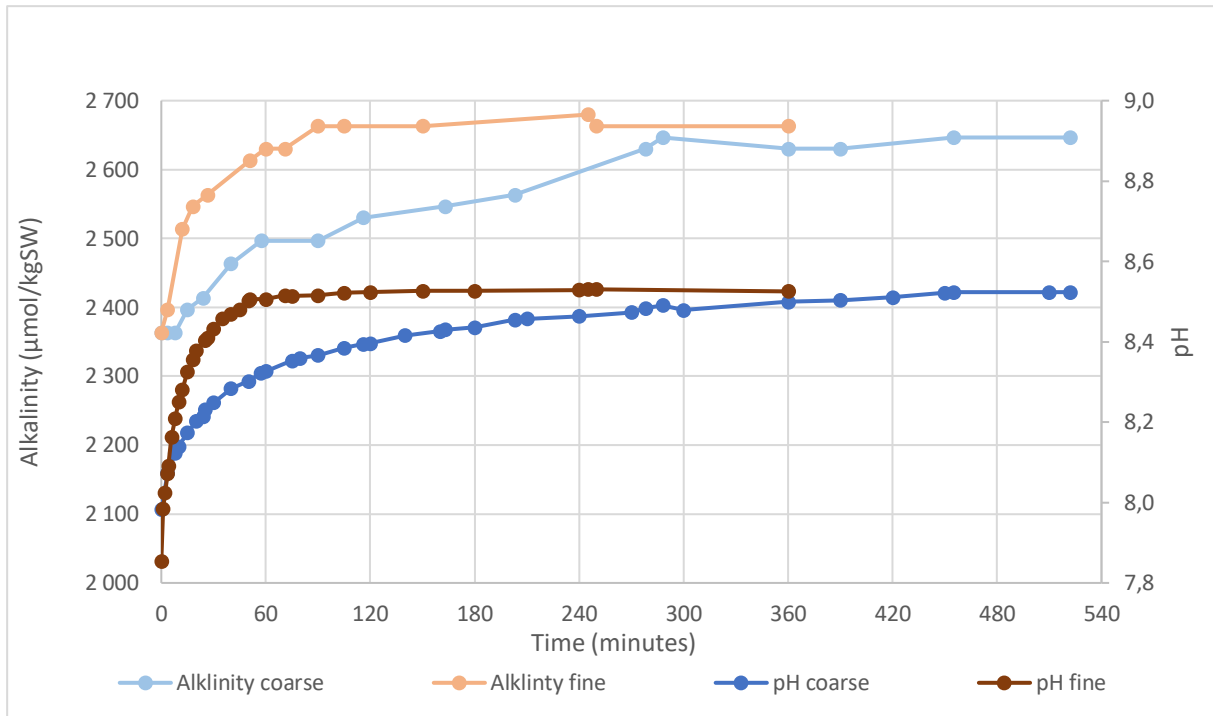


Figure 9 pH/alkalinity change from coarse and fine $\sim 0.01 \text{ g L}^{-1}$ CaO: Comparison of 0.1519 coarse CaO and 0.1508 fine CaO mixed with 15 L seawater at 14°C , 1 atm. Alteration in pH and TA happen quicker for fine vs coarse-grained CaO.

3.3 Results from different concentrations of CaO

3.3.1 Effect on pH from different concentrations of CaO

For each filtration 400 mL seawater was necessary. After collecting 20 such samples 8 L seawater from the original 15 L had then been removed. Adding on that number was the additional 15-25 mL used for ICP-MS in each collection. Although over half the original solution had been depleted sights of precipitate was still observable after the experiment was completed, figure 10.

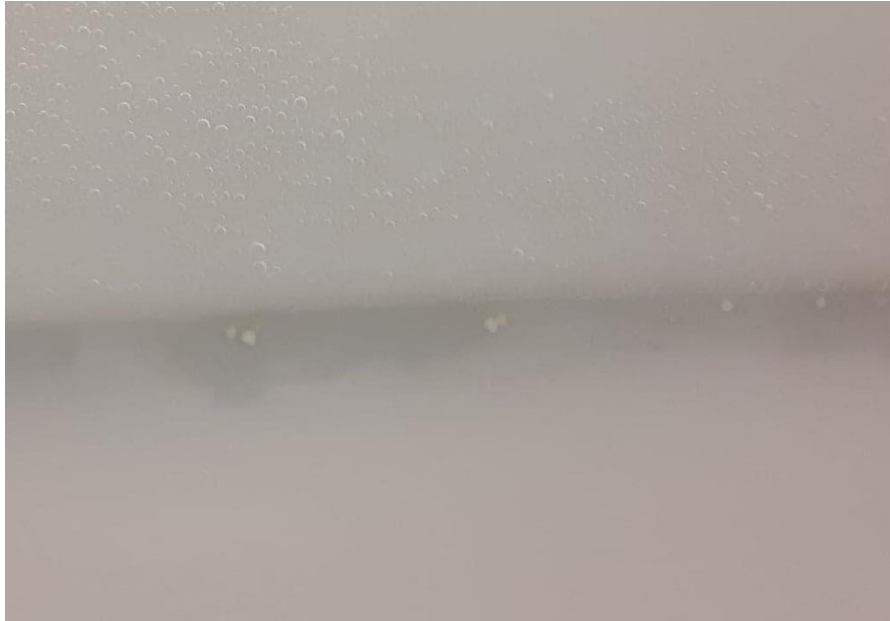


Figure 10 Precipitate after end of experiment: Precipitate was frequently seen, especially for higher doses of fine CaO. This picture was taken ~200 minutes after 0.2252 g fine CaO was mixed with 15 L seawater.

Measurement of pH for higher doses of fine CaO was performed separately for logistical reasons. Volume seawater was consequentially unchanged from original levels for these readings. Although increased values similarities can be observed in the rate the curve decline in regard to time. Both maximum pH values are recorded after 140 minutes with 8.79 and 8.91 for respectively ~ 0.015 - and ~ 0.02 g L⁻¹ CaO doses (appendix A). Overall change in pH value after 140 minutes is, 0.69 after ~ 0.01 g L⁻¹ CaO, 0.81 after ~ 0.015 g L⁻¹ CaO and 0.95 after ~ 0.02 g L⁻¹ CaO. While doses change approximately 0.075 g between them the difference in overall change between ~ 0.02 and ~ 0.015 g L⁻¹ CaO higher than for ~ 0.015 and ~ 0.01 g L⁻¹ CaO (0.14 and 0.12 units respectively).

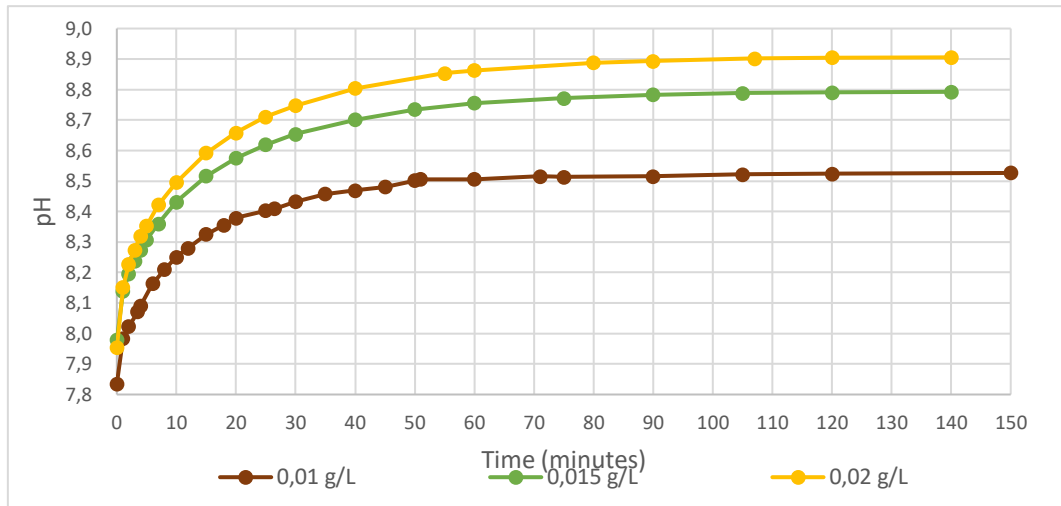


Figure 11 pH variation from three concentration fine-CaO in seawater: 0.1508-, 0.2256- and 0.3009 g fine CaO was mixed with 15 L seawater at 14°C, 1 atm and expected salinity at 33.6. Higher the dose of CaO, higher is the measured change. Average slope for the pH meter(A) was found to be 96.3 % for 0.1508 g experiment while it was 98.4 % for 0.2256- and 0.3009 g experiments. Dataset is presented in appendix A.

3.3.2 ICP-MS of filtrate

Analysis of filtrate was performed between one and two weeks after experiment completion. Of interest are ²⁵Mg and ⁴⁴Ca which similarities are pointed out in figure 12-15 and appendix D.

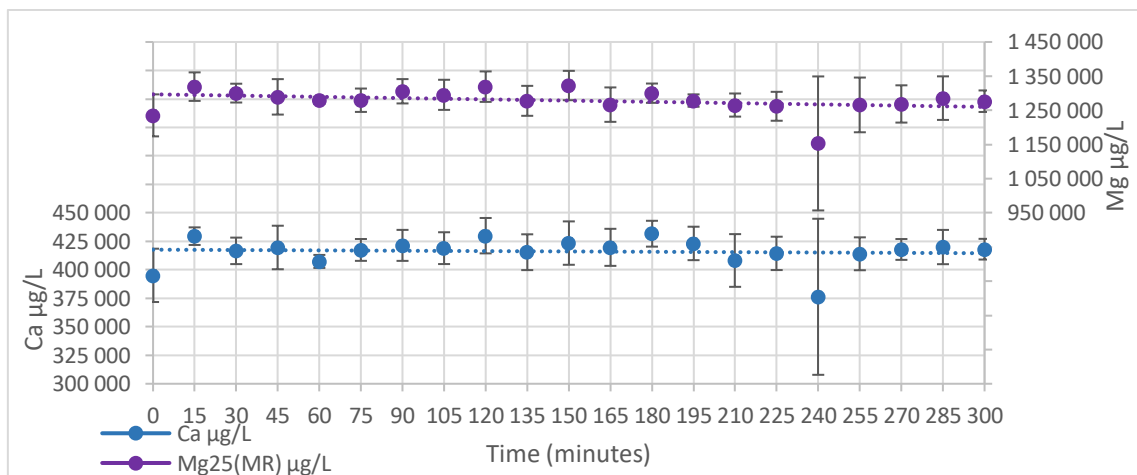


Figure 12 [Ca] and [Mg] after addition of ~0.01 g L⁻¹ coarse grained CaO: Filtrate prepared by 0.1516 g coarse-CaO mixed in 15 L seawater at 14°C, 1 atm. Two samples, after 60- and 240-minutes lack replicas and data represent only the one measurement. The amount of measured Ca and Mg has a slightly decreasing trend as time goes, but the average content for Ca and Mg after addition of CaO have increased 22 038- and 45 337 µg L⁻¹ respectively.

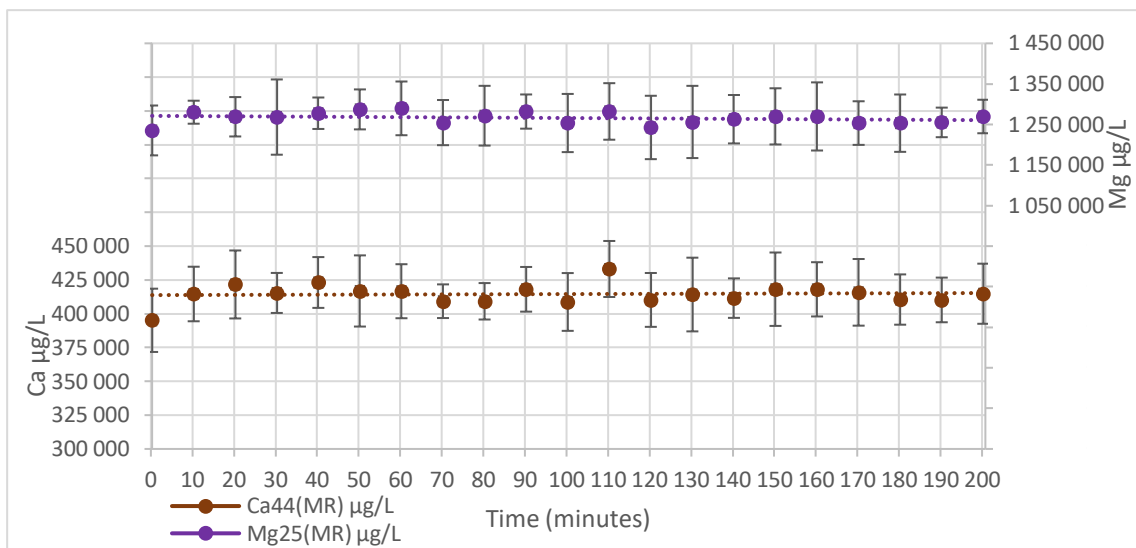


Figure 13 [Ca] and [Mg] after addition of $\sim 0.01 \text{ g L}^{-1}$ fine grained CaO: Filtrate prepared by 0,1502 g fine-CaO mixed in 15 L seawater at 14°C , 1 atm. Trends for Mg are here decreasing in regard to time while Ca is stable or slightly increasing, although both trends are minor. The average content, however, for Ca and Mg after addition of CaO have increased 20 363- and 32 153 $\mu\text{g L}^{-1}$ respectively.

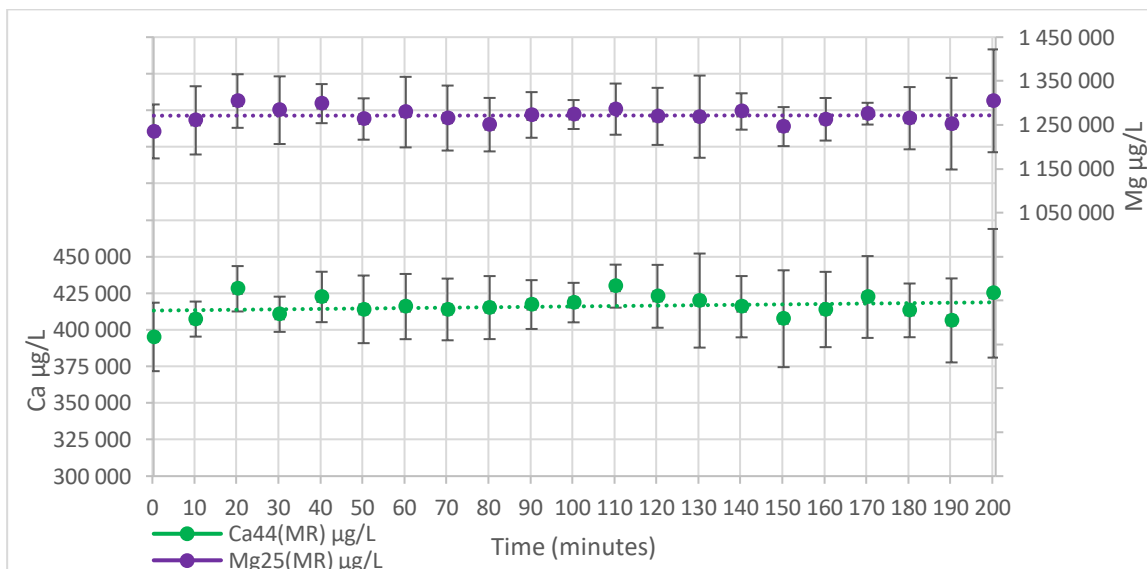


Figure 14 [Ca] and [Mg] after addition of $\sim 0.015 \text{ g L}^{-1}$ fine grained CaO: Filtrate prepared by 0.2252 g fine-CaO mixed in 15 L seawater at 14°C , 1 atm. Mg content are slightly increasing in regard to time while an even stronger increasing indication is seen for Ca. Like for $\sim 0.15 \text{ g}$ addition an increase between initial and average content after addition is observed with 21 874- and 38 068 $\mu\text{g L}^{-1}$ for Ca and Mg respectively

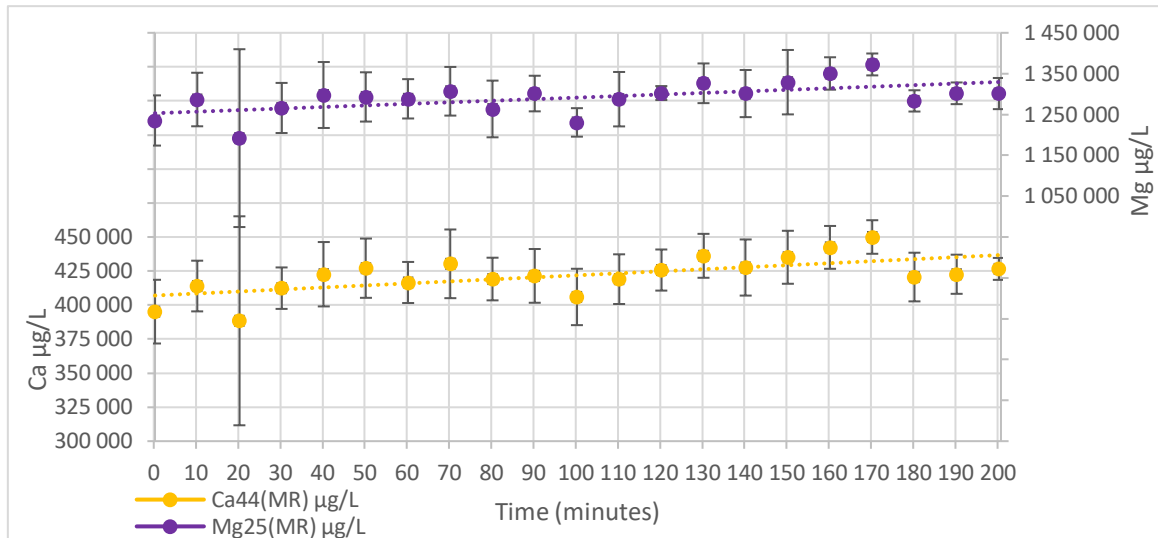


Figure 15 [Ca] and [Mg] after addition of $\sim 0.02 \text{ g L}^{-1}$ fine grained CaO: Filtrate prepared by 0.3002 g fine-CaO mixed in 15 L seawater at 14°C , 1 atm. The increase between initial and average content after addition is 28 021- and 58 803 $\mu\text{g/L}$ for Ca and Mg respectively.

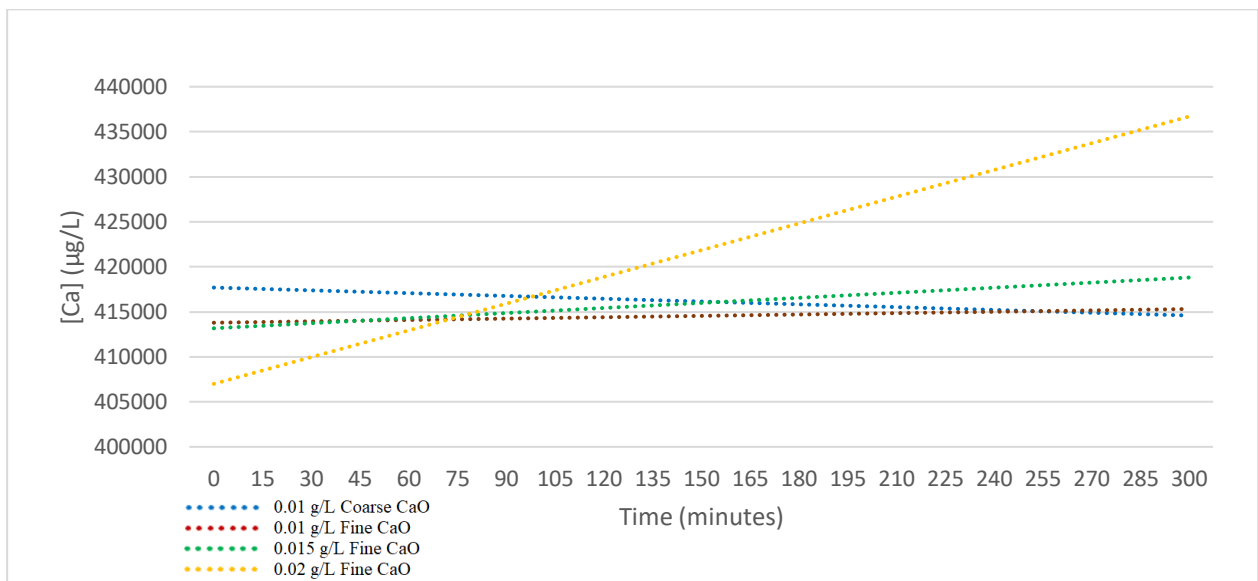


Figure 16 Calcium trends in solution after different CaO addition: Comparison calcium content in figure 12-15.

3.3.3 Particulate inorganic carbon formation

Particulate carbon formation can originate from both organic and inorganic sources. However, for the purpose in this study, focus was on the particulate inorganic carbon, PIC although presence of particulate organic carbon is obvious (about $40 \mu\text{g L}^{-1}$). The change in POC however is likely irrelevant compare to the formation of PIC during the experiment.

The carbon result presented here is based on 158 filtered samples stored 4-5 months in a desiccator before being analysed. Before analyses, the filters had to be divided and packed into two new tinfoil caps. As some samples lack duplicates, they are excluded in figures below but presented, along with data for the figures 19-23 in appendix E.

Coarse grained CaO compared to fine grained CaO have a smaller initial growth of PIC in the first 30 minutes as can be observed in figure 17, 18 and 21. Even though the maximum value particulate carbon in figure 17 is measured after 15 minutes as $140.1 \mu\text{g L}^{-1}$, $52.3 \mu\text{g}$ higher than before addition ($88.5 \mu\text{g L}^{-1}$). The average value is $86.4 \mu\text{g L}^{-1}$ which is higher than before addition while lowest measurement is found after 135 minutes at $67.7 \mu\text{g L}^{-1}$.

Fine grained CaO, figure 18, initial growth peaks after 10 minutes with $460.0 \mu\text{g L}^{-1}$ measured, $396.8 \mu\text{g}$ more than before addition. A decreasing trend for the measurements follows until 90 minutes ($102.4 \mu\text{g L}^{-1}$). Between 90- and 160-minutes development is flattened with an average value of $99.8 \mu\text{g L}^{-1}$ before a raise in the last three measurement.

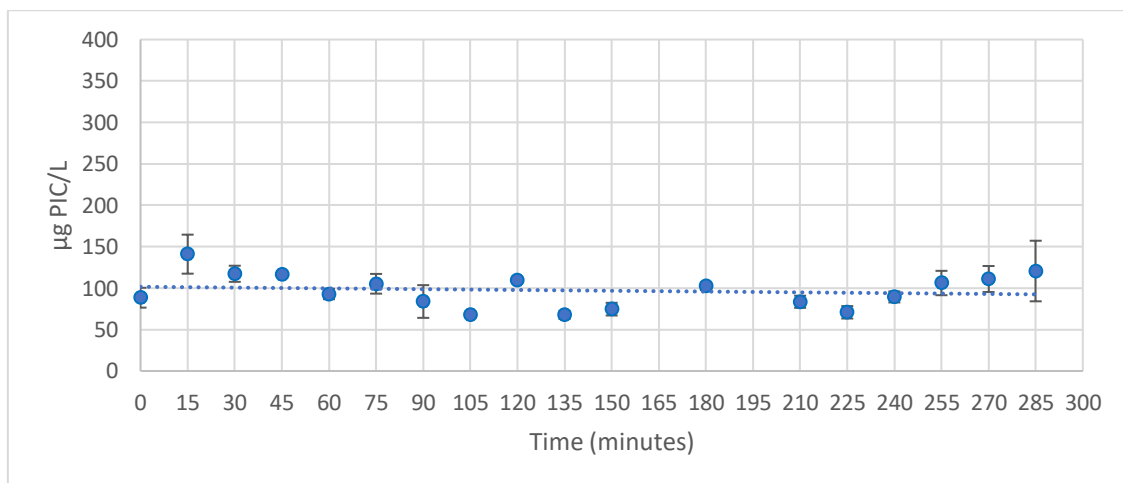


Figure 17 Particulate carbon after $\sim 0.01 \text{ g L}^{-1}$ coarse CaO addition: 0.1516 g coarse- CaO mixed in 15 L seawater at 14°C , 1 atm . Figure show PIC when POC is expected to be $40 \mu\text{g L}^{-1}$. A slight lowering trend is observed in particulate carbon after addition. Sample 13 (195 minutes) and 20 (300 minutes) have only one duplicate and not included in this figure. Sample 11 (165 minutes) is also excluded as a subsample of 11B(B) had a massively deviating value of $120 \mu\text{g}$. Excluded samples is however presented in appendix E.

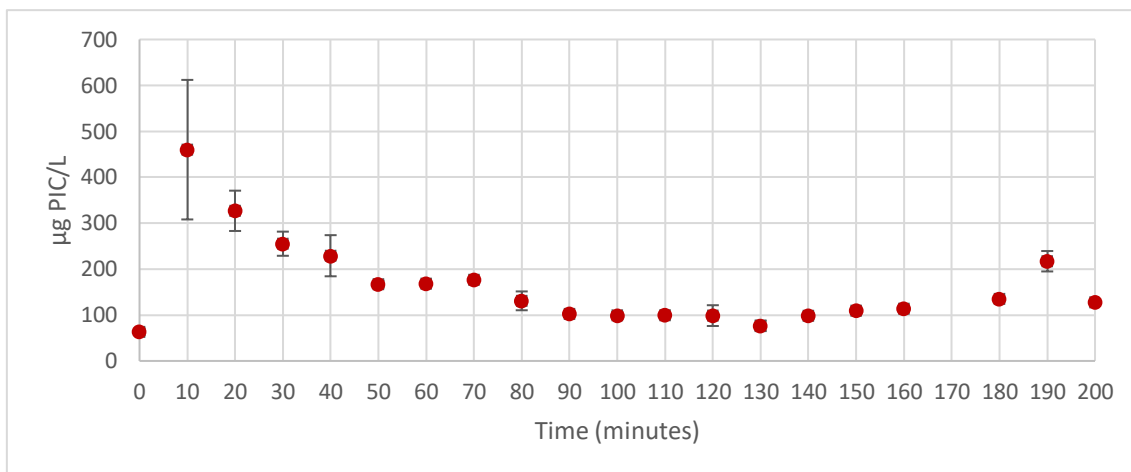


Figure 18 Particulate carbon after $\sim 0.01 \text{ g L}^{-1}$ fine CaO addition: 0.1502 g fine- CaO mixed in 15 L seawater at 14°C , 1 atm. Figure show PIC when POC is expected to be $40 \text{ } \mu\text{g L}^{-1}$. Beside the initial increased values an additional increment is found after 190 minutes. Sample 17 (after 170 minutes) have only one duplicate and not included in this figure but presented in appendix E.

When the amount of CaO added is raised the initial measurement is also more substantial as observed in figure 18-21. From addition of $\sim 0.015 \text{ g L}^{-1}$ CaO (figure 21) the maximum value PIC is found after 10 minutes as $613.2 \text{ } \mu\text{g L}^{-1}$, $549.9 \text{ } \mu\text{g}$ more than before addition. While after $\sim 0.02 \text{ g L}^{-1}$ CaO (figure 22) the maximum value PIC after 10 minutes is $1000.5 \text{ } \mu\text{g L}^{-1}$, additional $387.3 \text{ } \mu\text{g}$ higher than for $\sim 0.015 \text{ g L}^{-1}$. Like for $\sim 0.01 \text{ g L}^{-1}$ the values for $\sim 0.015 \text{ g L}^{-1}$ and $\sim 0.02 \text{ g L}^{-1}$ will decrease before flattening out. By comparing the steady values between 90-200(90-160 for $\sim 0.01 \text{ g L}^{-1}$) minutes for the different addition of fine CaO it is noticeable that higher amount added increase the average value, which is also observable in figure 23. The average value in this window is $99.7 \text{ } \mu\text{g}$ for $\sim 0.01 \text{ g L}^{-1}$, $123.9 \text{ } \mu\text{g}$ for $\sim 0.015 \text{ g L}^{-1}$ and $162.3 \text{ } \mu\text{g}$ for $\sim 0.02 \text{ g L}^{-1}$ which mean an average PIC increase per gram CaO of 3650-, 4046- and $4955 \text{ } \mu\text{g L}^{-1}$ respectively.

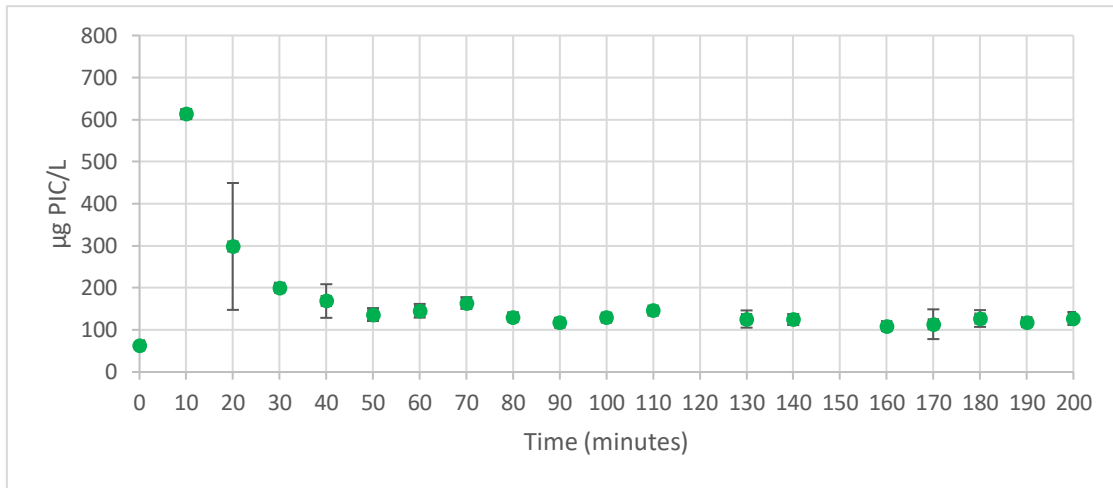


Figure 19 Particulate carbon after $\sim 0.015 \text{ g L}^{-1}$ fine CaO addition: 0.2252 g fine- CaO mixed in 15 L seawater at 14°C , 1 atm. Figure show PIC when POC is expected to be $40 \mu\text{g L}^{-1}$. Sample 12 (after 120 minutes) and sample 15 (after 150 minutes) have only one duplicate and not included in this figure but presented in appendix E.

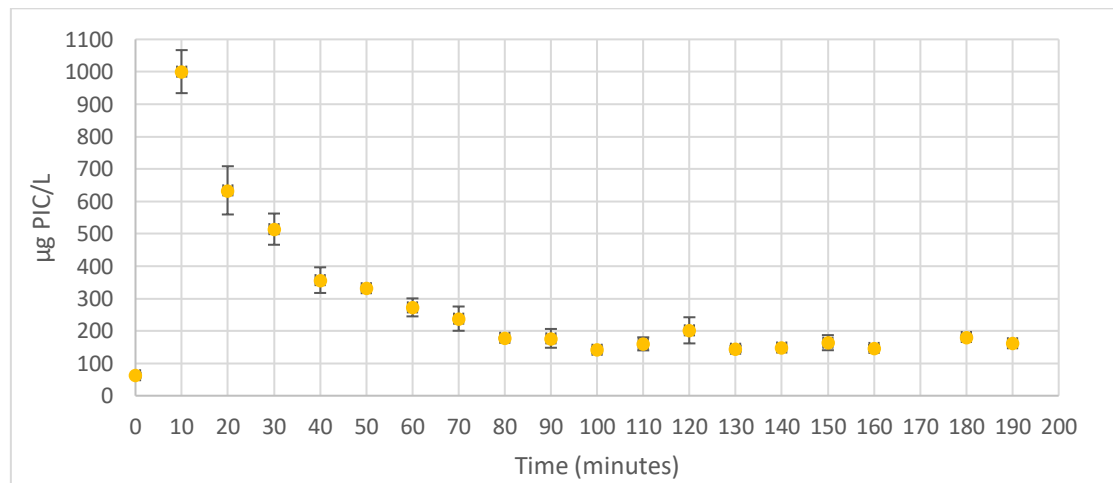


Figure 20 Particulate carbon after $\sim 0.02 \text{ g L}^{-1}$ fine CaO addition: 0.3002 g fine- CaO mixed in 15 L seawater at 14°C , 1 atm. Figure show PIC when POC is expected to be $40 \mu\text{g L}^{-1}$. Sample 17 (after 170 minutes) have only one duplicate and not included in this figure but presented in appendix E while sample 20 (after 200 minutes) have zero and therefore missing.

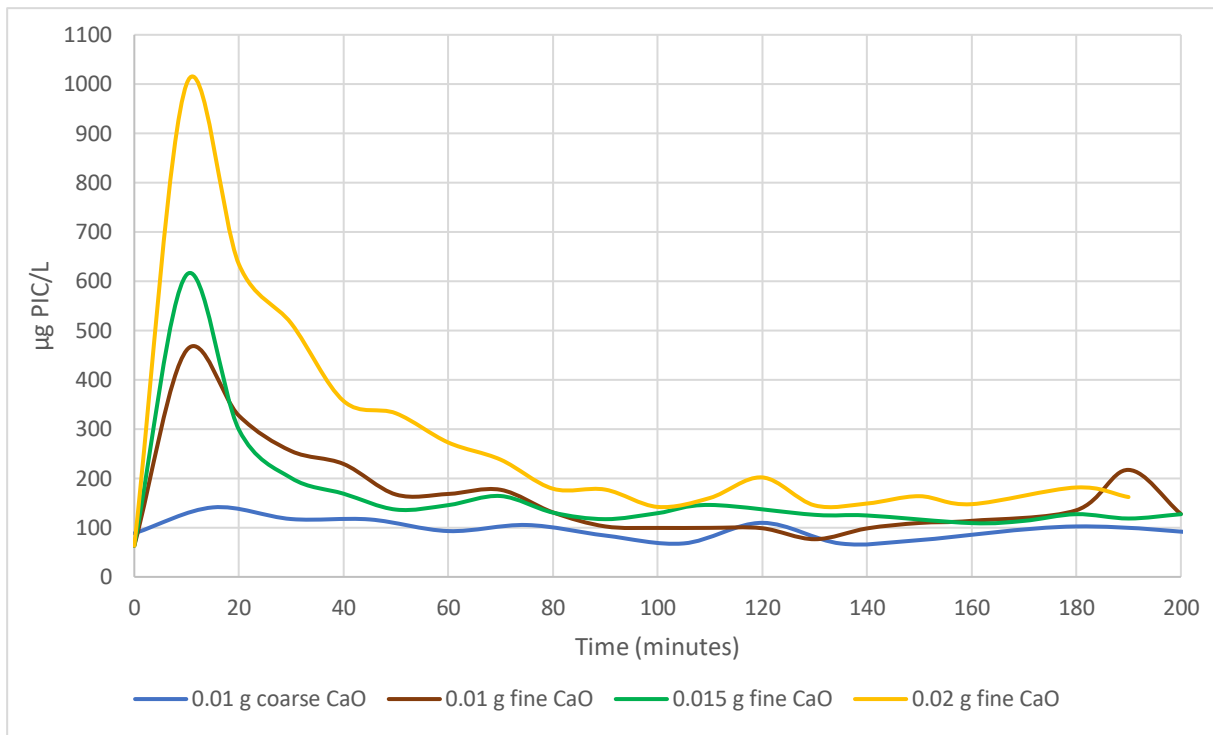


Figure 21 Comparison of particulate carbon formation from different grain and concentration of CaO:
Particulate carbon formation in figure 17-20, The figure shows immediate (within 10 minutes) carbon formation, with time the carbonate salt dissolve back. This trend was similar for all doses.

3.4 Duplicate XRF runs

Samples for this experiment unlike the rest had an electrostatic behaviour that lead to attachment to the petri dish walls. This behaviourally tendency was more frequent for trial B than for trial A. The lighter elements that the instrument could not detect, called BAL for balance was the biggest contributor with an average value of 86.53 % for both dataset (not counting blanks with average value of 99.41). After addition of CaO Ca % increased from 0.90 % (trial A) and 0.87 % (trial B) to 1.38 % (trial A) and 1.44 % (trial B) the first ten minutes, which was the maximum value collected from trial B. Maximum Ca % was for trial A was 1.41 % measured after 20 minutes. The average difference in values between trial A and trial B are 0.015 points. Other elements detected was Si, K, Zn, Al, Fe, Mn, Hg, Sr, Zr arranged in order of magnitude (dataset for elements is presented in appendix C).

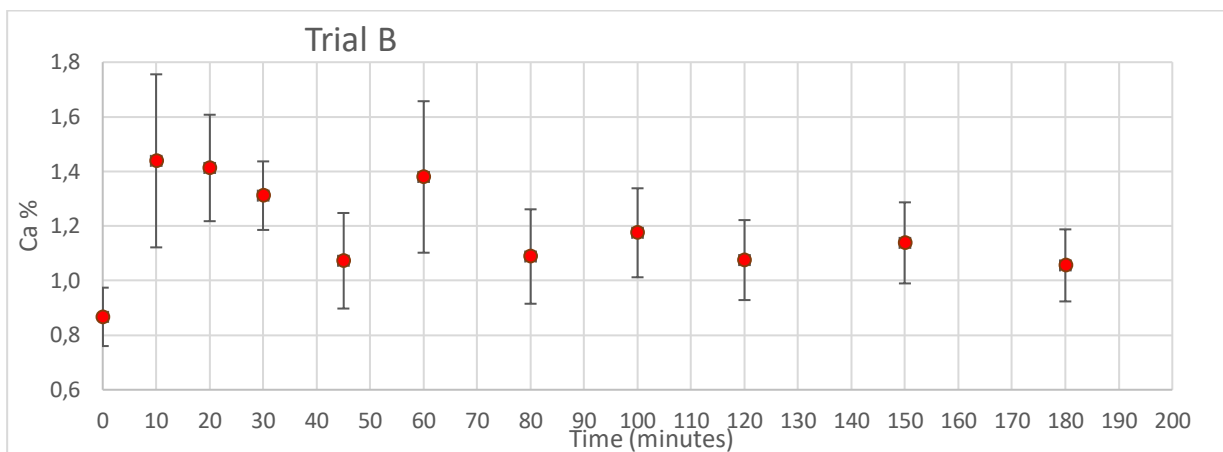
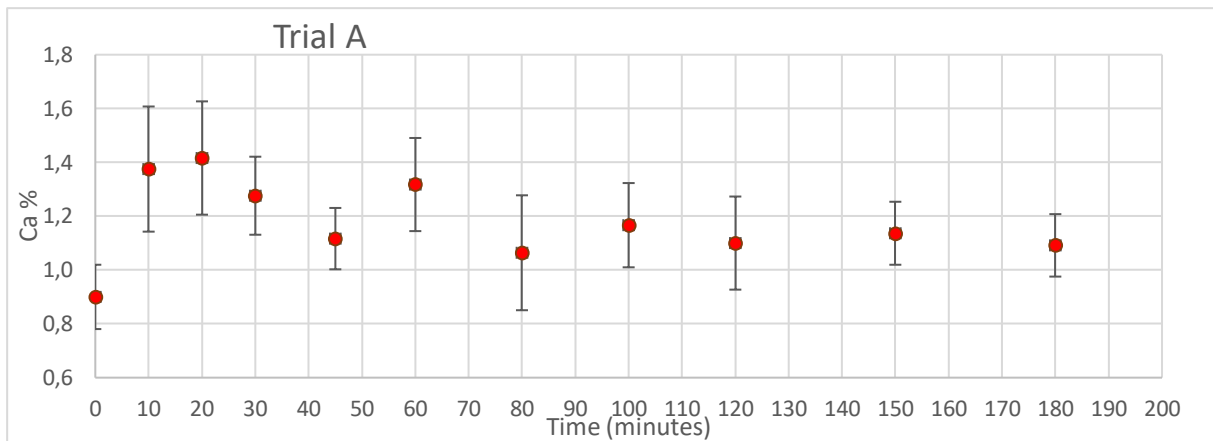


Figure 22 XRF solid Ca after $\sim 0.01 \text{ g L}^{-1}$ CaO addition (trial A)

Figure 23 XRF solid Ca after $\sim 0.01 \text{ g L}^{-1}$ CaO addition (trial B): Trial A and B for XRF measurement of 0,1505 fine CaO mixed with 15 L seawater at 14°C , 1 atm. Data for trial A and trial B is collected from 2 duplicates with the handheld instrument, NITON XRF Analyzer and accompanied software. Higher values of Ca % is detected on GFF filters after CaO addition.

4. DISCUSSION

4.1 Feedback on pH from different CaO addition

The wish to attain ~0.5 units pH alteration from the CaO addition was desired to both achieve measurable results and not deviate too much from what could realistically be applied in an in-situ operation. Like for Amundsen Gulf north of Canada that could reach a drop to pH of 7.8 by year 2100 in a business-as-usual scenario (Shadwick, Trull, Thomas & Gibson 2013). As knowledge on ocean acidification can confirm small changes of ocean pH can lead to many changes in chemical and biological processes in marine systems and species compositions (section 1.1).

The initial measurement of pH is a bit deviating as it stretches from 7.83 to 7.98 (in tank measurements) giving values lower than the 8.01 measured in Trondheimsfjorden by the Norwegian environment agency (Chierici et al. 2015). Usually the pH for NBS scale should be 0,1-0,15 units higher than for seawater scale which Chierici et al used to measure. The deviance might come from collection during various times while the lower values is expected as it was collected from 100 m depths. More importantly is the calibration and the not so well protected electrodes used that provide different values. NBS standard buffers used have low ionic strength, 0,1 unlike seawater with ionic strength 0,7 (equation 13). This causes significant changes in the liquid junction potential between calibration and measurements (Zeebe & Wolf-Gladrow 2001). Although specific pH values might be too low the change happening to pH is likely correct. After addition of 0.01 g L^{-1} , pH values rise up to ~8.5 for both fine and coarse CaO. Both the responses had similarities in magnitude and reaction fate but were larger and quicker for fine-grained than for coarse-grained CaO, as was expected based on their specific surface area and percentage active CaO seen in appendix F. Renforth et al suggested an optimal CaO diameter size between 50 and 100 μm for it to be dissolved within the mixed layer of the ocean (data based on dissolution in freshwater) (Renforth et al. 2013). Fine CaO grains in this thesis has a diameter between 0.2 and 0.8 mm and smaller grains would then lead to even rapider changes in pH. From the preliminary experiment and with different doses of fine CaO it is apparent that total change in pH and amount CaO added are not increasing uniformly. The change of pH is more extensive compared to doses as they increase. It is noticeable that observable precipitation also increased as dosage increased. From the pCO_2 values in the experiment (presented in appendix B) it can be expected that

actual total change in pH should be smaller for an in-situ experiment exposed to more invasive CO₂ lowering the pH (as seen in equation 8).

Calculation from CO₂sys macro spreadsheet show an initial total alkalinity of 2364 μEq L⁻¹ which is larger than average oceanic alkalinity (section 1.4). At 100 m depth the salinity is expected to be more or less stable but might be slightly lower or higher than the constant conditions presented in this thesis. The change however is likely to small to impact pH and DIC. More importantly is the effect of uncertain electrodes and the fact that the titration, which the calculation is based on went on to pH 3.7 instead of 4.5 in Dickson's definitions and therefore producing higher values (section 1.3). Actual values should therefore be carefully considered. The total change in alkalinity is however not necessarily wrong and more important for the scope of this study.

Conditions for each set of experiment may also vary as the length of time the water was stored before being used could be days up to weeks leaving still seawater the chance to settle. Seawater was additionally collected at different times in late autumn and spring causing seasonal varieties. Although the seawaters response to AOA seems invariant to when in the season the alkalinity is added (Lenton, Matear, Keller, Scott & Vaughan 2018).

4.2 Kinetic interpretations

From figure 7, 8 and 11 it is clear that the reaction between CaO and water can be followed by pH alteration. An attempt to determine the reaction order can by those reasons go on by comparing changes in [OH⁻] (equation 27 derived from equation 26) when different doses CaO is used (M. V. Ardelan, personal communication, April 5, 2019).

$$K_w = [\text{OH}^-][\text{H}^+] = 0,45 * 10^{-14} \text{ (for } 15 \text{ }^\circ\text{C, } 1 \text{ atm)} \quad 26$$

$$[\text{OH}^-] = 0,45 * 10^{-(14-\text{pH})} \quad 27$$

In figure 7 and 11 the pH alteration happens quickly and a plot for [OH⁻] against time should be applied before the reaction has completely stagnated (after around 60 minutes). In this interpretation it is apparent that the reaction rate change dependent on added concentration of CaO and a zeroth order reaction is not likely. This can also be concluded from figure 12-16 which the rate of calcium formation seems dependent on amount of added CaO.

From equation 23 and equation 9 we find equation 28 concerning OH^- , and the individual rates can be found by plotting the concentration against time, figure 24. By comparing the rate, equation 28 from the three reaction the reaction order can be interpreted by the slope of the plots.

$$\text{Rate} = \frac{1}{2} \frac{d\text{OH}}{dt}$$

28

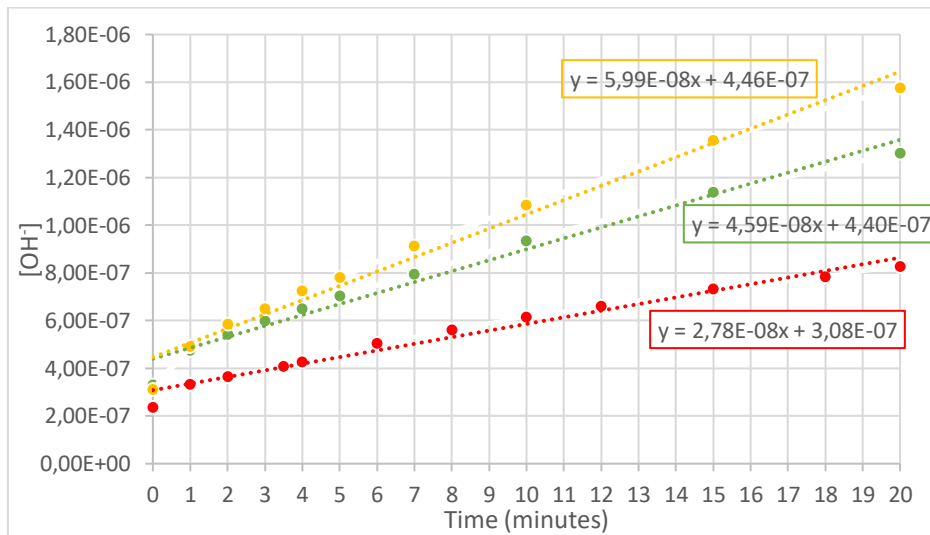


Figure 24 Changes in $[\text{OH}^-]$ from different concentrations of CaO : 0.1508-, 0.2256- and 0.3009 g fine CaO was mixed with 15 L seawater at 14°C , 1 atm and expected salinity at 33.6. The first 20 minutes of the reaction was chosen because of the almost linear reaction rate. By finding the $d\text{OH}/dt$ from different dosage reaction order can be determined.

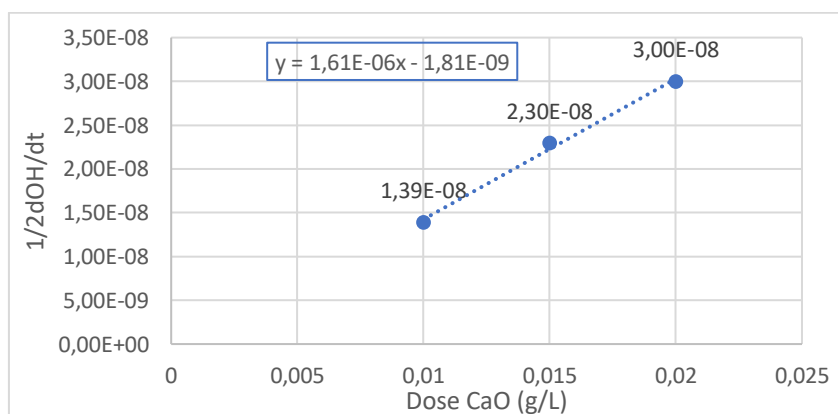


Figure 25 Comparing rates of formation from three doses of CaO : From equation 23: $-\text{dCaO}/dt = 1/2 d\text{OH}/dt$. Linear relationship means first order while a quadratic relationship means second order.

The reaction order can by these assumptions be defined as first order and the rate follow the concentration of CaO, equation 29.

$$\text{Rate} = k [\text{CaO}] = 1.61 * 10^{-6} [\text{CaO}] \text{ (at 14-15 } ^\circ\text{C, 1 atm, salinity } \sim 33.6 \text{ ‰)} \quad 29$$

Determination of kinetics in seawater can be problematic as ions interfere, organic matter interacts and limiting knowledge of the complexity of the reaction in question (section 1.11). This is also the case for using $[\text{OH}^-]$ when any resistance to pH in the solution change the result. While equation 29 may not be transferable for different sets of conditions it can provide knowledge in these particular conditions. However, when pCO_2 are present days values and total amount pH units has decreased this rate will also be altered.

4.3 Alkalinity and DIC

Presented results support earlier researched ideas of CaO addition as a mean to increase the oceans total alkalinity. Although values for DIC and pCO_2 (appendix B) should be consider with caution as earlier mention the change in DIC are not increasing, but instead show a minor decline. This contradict with Kheshgi estimates for an increase in DIC content of 0.89 mole per mole alkalinity added (Kheshgi 1995). For AOA to participate in removing CO_2 from the atmosphere, DIC must increase as the alkalinity increase which effect is expected for several global AOA modelling efforts (González & Ilyina 2016; Ilyina et al. 2013; Lenton et al. 2018). A main limitation in presented experiments is the level of pCO_2 that is diminishing in the closed tank, which Kheshgi substantiates with a constant $\text{pCO}_2 = 350 \mu\text{atm}$ in his estimates. From calculation the pCO_2 in the tank has diminished 4 to 6 times from start to end of experiment (appendix B). If the experiment was exposed to a constant present day pCO_2 the influx of CO_2 between the atmosphere and surface water interference is expected to increase the DIC content as predicted in the several AOA modelling and in equation 10 proposed by Kheshgi.

As little new carbon was available to push the carbon equilibrium, no apparent change can be expected, but rather a decline can be argued for as precipitate of what is likely CaCO_3 was observed in the bottom of the tank after experiments. For both fine and coarse CaO the Ω_{Ca} increased from ~ 2 to ~ 8 (appendix B) which are still lower than the 20-25 times supersaturation required for abiotic spontaneous precipitation (Renforth & Kruger 2013). Locally elevated values could explain observation as well as the decrease in DIC occurring

the first minutes illustrated in table 3 and 4. Peaks after 10-30 minutes for XRF (figure 22 and 23) and infrared absorption (figure 17-21) seems also to support increased CaCO_3 precipitation in these early stages of the reaction. CaCO_3 precipitate could potentially lead to a decrease in alkalinity by two moles for each mole CaCO_3 , if formed from dissolved CO_3^{2-} . This decline in alkalinity, although could be relatively small is not observed (table 3 and 4, figure 9 and appendix B).

Based on calculation by the CO2sys macro spreadsheet an increased pH from CaO addition shifts the composition of inorganic carbon species (seen in Bjerrum plot, figure 1. Decrease of $[\text{HCO}_3^-]$ would also decrease the total alkalinity but is countered by increased values of $[\text{CO}_3^{2-}]$, $[\text{B}(\text{OH})_4^-]$, and $[\text{OH}^-]$. Since CO_3^{2-} contribute with 2 mole TA the alkalinity can increase despite total DIC staying unchanged. For an open system experiment $[\text{HCO}_3^-]$ is thought to increase by 1.62 moles per mole CaO (reaction 10). This result could be because this experiment is in a closed system deprived by influx of CO_2 . Atmospheric CO_2 diffusion along with precipitation of carbonate minerals is the main source and sink for DIC, thus for DIC to increase more CO_2 must be available. Invasive CO_2 also acidify meaning lower total pH alteration and reverse the shift in inorganic carbon composition to higher $[\text{HCO}_3^-]$. Since alkalinity is conservative measurement the DIC should thereby increase. Since seawater used is slightly less saline than in the suggestion presented by Khesigi (34.87 vs presumably ~33.6 ‰) the proportion of $[\text{CO}_3^{2-}]$ compared to $[\text{HCO}_3^-]$ is also higher (section 1.2).

4.4 Dissolution and precipitation

By filtrating the samples through a 0.2 μm filter should mean $[\text{Ca}]$ as well as in aqueous form will be colloidal or nanoparticle but will for simplicity be regarded as dissolved. GFF filters used retain down to 0.7 μm leaving a gap appears between 0.2- and 0.7 μm which fate of calcium or carbonates cannot be determined by this study. Even though $[\text{OH}^-]$ was used to determine kinetic it is less telling for $[\text{Ca}]$ when CaCO_3 precipitate and other formations remove it as a dissolved product. This case of carbonate-precipitate is observed in figure 17-23. However, the extent of how much is CaCO_3 compare to other carbonates cannot be determined in this study. Since saturation state for both calcium and magnesium evolve even more oversaturated, seen in appendix B it is likely MgCO_3 and other similar carbonates contribute to peaks measured. Although contribution from organic compounds will not be discussed further here it cannot be excluded.

Calculation made on saturation states for calcium and magnesium is based on alkalinity measurements and they are similar in their development. It would therefore be natural to predict PIC to follow the same rate. The deviating behaviour seen however in figure 17-23 could be a result of local high saturation values close to dissolving CaO particles causing carbonate precipitation before gradually dissolving again as these local environments seize. Elevated pH increases the proportion of CO_3^{2-} to other inorganic carbon species. Although oversaturation means the value of K is lower than for its corresponding products in equation 30 and 31 (section 1.5) an increase of $[\text{CO}_3^{2-}]$ would usually mean a decrease of $[\text{Ca}^{2+}]$ and $[\text{Mg}^{2+}]$.

$$K_{sp} = [\text{Ca}^{2+}] \times [\text{CO}_3^{2-}] \quad 30$$

$$K_{sp} = [\text{Mg}^{2+}] \times [\text{CO}_3^{2-}] \quad 31$$

This can argue for the modest initial increase of dissolved calcium seen in figure 12-15. If carbonate compounds gradually dissolve again as earlier predicted accompanied by only minor pH alteration seen in figure 11 (after 30-40 minutes) steady increased values of $[\text{Mg}]$ and $[\text{Ca}]$ will derive from the dissolution and observed in figure 15. The correlation between calcium and magnesium seen in figure 12-15 and figure 30 (appendix D) further indicate the $[\text{Ca}]$ and $[\text{Mg}]$ is controlled by $[\text{CO}_3^{2-}]$ and therefore pH and dissolution/precipitation of carbonate compounds. From figure 10 it is clear however that precipitation was observed after some experiments which leaves the possibility that early formed PIC coagulates and sink to the bottom of the tank escaping the sampling procedure.

The average formation of PIC between 90-200 minutes (90-160 minutes for 0.01 g L^{-1}) is more extensive when dosage CaO is increased which was also noticed for pH measurement. This will only be the case if the last three measurements in figure 20 (90-200 minutes for 0.01 g L^{-1}) is excluded and should therefore be cautionary considered. Increased dosage would however increase the initial peak of PIC found after 10-15 minutes. The extend of this peak is important as abiotic precipitation could settle directly onto organisms and cause optic stress (section 1.7). Although the total change in pH and alkalinity is comparable for coarse- and fine grained 0.01 g L^{-1} (figure 11) the initial peak for coarse CaO are minor compared to fine (figure 19 and 20).

Estimated mean oceanic $[\text{Ca}]$ is $10.28 \text{ mmol Kg}^{-1}$ (Nozaki 2001). In the batch of seawater used for non-dispersive infrared absorption and ICP-MS analyses the $[\text{Ca}]$ was $9.86 \pm 0.58 \text{ mmol Kg}^{-1}$. The lower value is expected when salinity was presumably lower, $\sim 33,6$

against 35 used for the mean oceanic estimate. In the final measurement seen in table 5, [Ca] have increased between 5 and 8 % for the different additions. Alkalinity is closely linked to the oceans charge balance (figure 3) and the imbalance that has driven the increased total alkalinity presented in this study seems to stem from enhanced [Ca] and [Mg]. Although calcium is mostly regarded as a conservative element in the ocean uncertainty arise from how organisms will cope with enhanced exposure (section 1.7).

Table 2 Final calcium concentration (200 minutes for fine CaO and 300 minutes for coarse) after addition of CaO under 33.6 salinity, 14°C, 1 atm (appendix D).

| <i>Initial addition</i> | <i>Final calcium concentration</i> |
|------------------------------------|------------------------------------|
| 0.010 g L ⁻¹ coarse CaO | 10.43 ± 0.23 mmol Kg ⁻¹ |
| 0.010 g L ⁻¹ fine CaO | 10.35 ± 0.55 mmol Kg ⁻¹ |
| 0.015 g L ⁻¹ fine CaO | 10.60 ± 1.10 mmol Kg ⁻¹ |
| 0.020 g L ⁻¹ fine CaO | 10.64 ± 0.20 mmol Kg ⁻¹ |

A strong indication for PIC detected stems from CaCO₃ can be verified by XRF measurement, figure 22 and 23. This also verify XRF as a tool to measure CaCO₃ precipitation development in-situ. The XRF-setup used in this study can however be improved using a more specialized container utilize vacuum or helium. Light elements are harder to detect with used equipment and is probably the reason why MgCO₃ fell below the detection limit. Other elements over the detection limit of interest like iron and strontium (table 13 and 14 appendix C) have no clear development indicating they stay unchanged.

4.5 Limitations, challenges and further investigations

Presented measurements and samplings accuracy is limiting by imprecise equipment, standards and human errors. They can be improved with using a more precise automatic system for pH, TA and temperature measurements. An automatic system could also be useful for following pCO₂ and supply more frequent measurements. A limitation in this study is the diminishing pCO₂, discussed in section 4.3 in this closed system affecting the total pH change and thereby the determined kinetics (section 4.2). The CO₂ sequestering potential is therefore not observed. For AOA (OL in this case) to be effective for sequestering it must increase DIC

in the ocean which was not observed in this study (table 3 and 4). An assessment of CaO addition in a open system with constant $p\text{CO}_2$ condition should therefor be conducted to conclude AOA's potential for CO_2 sequestering.

More studies assessing biological response concerning AOA and OL is also needed. Of importance is how organisms are affected by increased $[\text{HCO}_3^-]$ (presumably), $[\text{CO}_3^{2-}]$, $[\text{Ca}^{2+}]$ and other elements indirectly altered by the addition of CaO, like $[\text{Mg}^{2+}]$ (section 1.7 and 4.4). Abiotic precipitation of CaCO_3 , possible observed in figure 21 is unwanted as it both cause stress to organisms and reduce the AOA impact. The precipitation magnitude from fine grained seem stronger than for coarse grained, but coarse grained (diameter between 0.5-2.5 mm) might be to large to dissolve in the mixed layer thereby minimizing its AOA potential (Renforth et al. 2013). The impact of temperature may be another stress moment. Although the temperature increase was not obvious by the level of equipment used in this study (section 3.1), it is expected as seen in appendix F and presented in section 1.7. An alternative oxide could be MgO, though not as available for mining but is less exothermic in contact with water (section 1.7). An additional alternative not covered by this study is the how the effect would be if $\text{CaO}_{(s)}$ was dissolved to $\text{CaOH}_{(aq)}$ before addition. This alternative should be investigated if temperature is a mayor stress factor.

The total alkalinity difference from coarse- and fine CaO addition (appendix B) leads to respectively 1.59 mole and 1.68 mole TA per mole CaO added ($0.01 \text{ g L}^{-1} \text{ CaO}$). Fine grained CaO is then in the range of the 1.6 to 1.8 TA per mole CaO predicted by Ilyina et al. This mean OL can potentially sequestrate more CO_2 per CO_2 emitted in production (1.65 mole, equation 10, compare to 1 mole, equation 11) without CCS technology. If the global production of CaO (283 million tons, 2007) was used for OL without CCS this would potentially sequester 0.15 Gt CO_2 (fine CaO used in this experiment). If CCS technology is implemented 100 % in the production the potential is 0.37 Gt CO_2 . AOA effectiveness to sequester CO_2 is therefore determined by complimentary CCS technology. The flue gas from the production contain however high $[\text{CO}_2]$ and might be suited for this technology (section 1.8). Although AOA can isolate this extra CO_2 in a long-term perspective the contribution made from the 2007 CaO production makes a small impact on the global emissions. 0.37 Gt amounts to 1 % of the projected annual emission for 2018 (37.2 Gt) which has risen over 2 % from the 2017 emissions (Le Quéré et al. 2018). Complementary emissions from heating, transportation and mining will additionally lower the CO_2 sequester potential.

4.6 Conclusion

Addition of CaO has been proven in this study to increase TA and pH in seawater. The reaction rate has been shown to follow first order characterization. This is apparent from changes in pH, and the PIC formation which unfolds the first 10-20 minutes after addition of different CaO doses. The extend of the peak could be important in OL contexts as it might have biological consequences. An in-situ PIC measurement technic could therefore be useful. XRF, although capacity for improvement, has here shown its potential.

The precipitated carbonate minerals seem to dissolve again but higher dosage results in higher average PIC after the imminent peak. Increased dosage also leads to higher [Ca] and [Mg], which elements show a correlative tendency.

For different grain size CaO the absolute pH and alkalinity difference is comparable but coarse grained showed a slower pH rate and only a small PIC precipitation was observed. This makes coarse CaO a gentler OL-alternative compare to fine CaO, although sinking rate should be considered.

A main limitation in this study is the diminishing $p\text{CO}_2$ and calculations did not conclude with enhanced DIC. OL potential to sequester CO_2 however is expected as alkalinity increased 1.68 mole (0.01 g L^{-1} fine CaO) per mole CaO. Effectiveness is however closely linked with CCS, emissions from mining, transportations and heating and scope of production. There is necessary to increase the production (2007 production) substantially for it to provide a real impact on global emission.

To reverse acidification is the main reason for considering CaO addition and it can be proven valuable for organisms depended on making calcareous organs and shells. A global scale could raise the ocean pH to pre-industrial values and potentially store CO_2 in the process. It could also be applied locally for especially vulnerable aquatic systems. These systems, subject to strong acidification makes it important to consider geoengineering. Not only because how the ocean reacts upon the addition of alkalinity, like CaO, but also how it reacts in a business-as-usually scenario.

Reference

- Alvarez, D., & Abanades, J. C. (2005). Pore-size and shape effects on the recarbonation performance of calcium oxide submitted to repeated calcination/recarbonation cycles. *Energy & Fuels*, 19(1), 270-278.
- American Water Chemicals (AWC), Inc. (2019) What is the relationship between pH and alkalinity? How are they different? How does temperature affect them? (n.d.). Retrieved March 19, 2019, from <https://www.membranechemicals.com/en/faqs/relationship-ph-alkalinity-different-temperature-affect/>
- Baird, C., & Cann, M. (2012). *Environmental chemistry* (5th ed.). New York: W.H. Freeman and company.
- Bobicki, E. R., Liu, Q., Xu, Z., & Zeng, H. (2012). Carbon capture and storage using alkaline industrial wastes. *Progress in Energy and Combustion Science*, 38(2), 302-320.
- Brezonik, P. (2018). *Chemical kinetics and process dynamics in aquatic systems*. Routledge.
- Chen, D. M. C. F., Frame, D., Mahowald, N., Winther JG. (2013). *Climate Change 2013: The Physical Science Basis. IPCC Fifth assessment report, Intergovernmental panel on climate change*. from: http://www.ipcc.ch/pdf/assessment-report/ar5/wg1/WG1AR5_Chapter01_FINAL.pdf
- Chierici, M., Skjelvan I., Norli M., Lødemel H.H., Lunde L.F., Sørensen K., ... & Børshheim K.Y. 2015. Monitoring ocean acidification in Norwegian waters in 2014, Rapport, Norwegian Environment Agency, M-354|2015.
- Clark, J. (2013, May). Equilibrium Constants and Le Chatelier's Principle. Retrieved March 19, 2019, from <https://www.chemguide.co.uk/physical/equilibria/change.html>
- Connell, S. D., Doubleday, Z. A., Hamlyn, S. B., Foster, N. R., Harley, C. D., Helmuth, B., ... & Russell, B. D. (2017). How ocean acidification can benefit calcifiers. *Current Biology*, 27(3), R95-R96.
- Dickson, A. G. (1981). An exact definition of total alkalinity and a procedure for the estimation of alkalinity and total inorganic carbon from titration data. *Deep Sea Research Part A. Oceanographic Research Papers*, 28(6), 609-623.

- Feng, E. Y., Keller, D. P., Koeve, W., & Oschlies, A. (2016). Could artificial ocean alkalization protect tropical coral ecosystems from ocean acidification?. *Environmental Research Letters*, 11(7), 074008.
- Feng, E. Y., Koeve, W., Keller, D. P., & Oschlies, A. (2017). Model-Based Assessment of the CO₂ Sequestration Potential of Coastal Ocean Alkalinization, *Earth's Future*, 5, 1252–1266, <https://doi.org/10.1002/2017EF000659>
- Frommel, A. Y., Maneja, R., Lowe, D., Malzahn, A. M., Geffen, A. J., Folkvord, A., ... & Clemmesen, C. (2012). Severe tissue damage in Atlantic cod larvae under increasing ocean acidification. *Nature Climate Change*, 2(1), 42.
- Gebremariam, K. F. Presentation on “XRF training” at NTNU 19.11-20.11 2018
- González, M. F., & Ilyina, T. (2016). Impacts of artificial ocean alkalization on the carbon cycle and climate in Earth system simulations. *Geophysical Research Letters*, 43(12), 6493-6502.
- Grasa, G., Martínez, I., Diego, M. E., & Abanades, J. C. (2014). Determination of CaO carbonation kinetics under recarbonation conditions. *Energy & Fuels*, 28(6), 4033-4042.
- Gupta, H., & Fan, L. S. (2002). Carbonation– calcination cycle using high reactivity calcium oxide for carbon dioxide separation from flue gas. *Industrial & engineering chemistry research*, 41(16), 4035-4042.
- Hansson, L., & Gattuso, J.-P. (2011). *Ocean Acidification*. Oxford [England]: OUP Oxford.
- Ilyina, T., Wolf-Gladrow, D., Munhoven, G., & Heinze, C. (2013). Assessing the potential of calcium-based artificial ocean alkalization to mitigate rising atmospheric CO₂ and ocean acidification. *Geophysical Research Letters*, 40(22), 5909-5914.
- International Energy Agency, IEA. (2017). *World Energy Outlook 2017*. From <http://www.iea.org/weo2017/>
- Keeling, C. D., Piper, S. C., Bacastow, R. B., Wahlen, M., Whorf, T. P., Heimann, M., & Meijer, H. A. (2019). Exchanges of atmospheric CO₂ and ¹³CO₂ with the terrestrial biosphere and oceans from 1978 to 2000. I. Global aspects, *SIO Reference Series*, No. 01-06, Scripps Institution of Oceanography, San Diego, 88 pages, 2001.

- Kheshgi, H. S. (1995). Sequestering atmospheric carbon dioxide by increasing ocean alkalinity. *Energy*, 20(9), 915-922.
- Köhler, P., Hartmann, J., & Wolf-Gladrow, D. A. (2010) Geoengineering potential of artificially enhanced silicate weathering of olivine. *Proceedings of the national academy of science of the united states of America*, 107, 20228-20233.
<https://doi.org/10.1073/pnas.1000545107>
- Le Quéré, C., Andrew, R. M., Friedlingstein, P., Sitch, S., Hauck, J., Pongratz, J., ... & Zheng, B.: Global Carbon Budget 2018, *Earth Syst. Sci. Data*, 10, 2141-2194,
<https://doi.org/10.5194/essd-10-2141-2018>, 2018
- Lenton, A., Matear, R. J., Keller, D. P., Scott, V., & Vaughan, N. (2018). Assessing carbon dioxide removal through global and regional ocean alkalization under high and low emission pathways. *Earth System Dynamics*, 9, 339-357.
- Ma, C., You, K., Ji, D., Ma, W., & Li, F. (2015). Primary discussion of a carbon sink in the oceans. *Journal of Ocean University of China*, 14(2), 284-292.
- Manahan, S. E. (2017). *Environmental chemistry* (10th ed.). Boca Raton: CRC Press.
- McGee, M. 2018, ProOxygen (2018, 20-2015). "CO2 earth." Retrieved 08.02.2018, from <https://www.co2.earth/>.
- Miller, M. M. (2007). "2007 Minerals Yearbook, Lime." Retrieved 08.02, 2018, from <https://minerals.usgs.gov/minerals/pubs/commodity/lime/myb1-2007-lime.pdf>.
- Millero, F. J., Lee, K., & Roche, M. (1998). Distribution of alkalinity in the surface waters of the major oceans. *Marine Chemistry*, 60(1-2), 111-130.
- Mollica, N. R., Guo, W., Cohen, A. L., Huang, K. F., Foster, G. L., Donald, H. K., & Solow, A. R. (2018). Ocean acidification affects coral growth by reducing skeletal density. *Proceedings of the National Academy of Sciences*, 115(8), 1754-1759.
- Morse, J. W., & Mackenzie, F. T. (1990). *Geochemistry of sedimentary carbonates* (Vol. 48). Elsevier
- Norwegian Mapping Authority (n.d.) [Trondheimsfjorden] retrieved January 17, 2019 from: <https://www.norgeskart.no/#!?project=norgeskart&layers=1003&zoom=9&lat=70419>

[40.73&lon=257999.87&sok=trondheimsfjorden&markerLat=7044400.643706512&markerLon=258402.16913286448&panel=searchOptionsPanel](https://www.britannica.com/entry/40.73&lon=257999.87&sok=trondheimsfjorden&markerLat=7044400.643706512&markerLon=258402.16913286448&panel=searchOptionsPanel)

- Nozaki, Y. (2001). Elemental distribution: overview. A derivative of Encyclopaedia of Ocean Science, 2nd edition
- Paquay, F. S., & Zeebe, R. E. (2013). Assessing possible consequences of ocean liming on ocean pH, atmospheric CO₂ concentration and associated costs. *International Journal of Greenhouse Gas Control*, 17, 183-188
- Rafferty, J. P., 2011. "Ocean acidification" In Encyclopædia Britannica. Retrieved (20.04.2019) from <https://academic.eb.com/levels/collegiate/article/ocean-acidification/570924>
- Renforth, P., Jenkins, B. G., & Kruger, T. (2013). Engineering challenges of ocean liming. *Energy*, 60, 442-452.
- Renforth, P., & Kruger, T. (2013). Coupling mineral carbonation and ocean liming. *Energy & Fuels*, 27(8), 4199-4207.
- Riebesell, U., Fabry, V. J., Hansson, L., Gattuso, J-P. (2010). Guide to best practices for ocean acidification research and data reporting., International Atomic Energy Agency, IAEA from https://www.iaea.org/ocean-acidification/download/OA%20guide/OA-Guide_Ch1_20100518.pdf.
- Rosa, R. & B. A. Seibel (2008). Synergistic effects of climate-related variables suggest future physiological impairment in a top oceanic predator. *Proceedings of the National Academy of Sciences* 105(52): 20776.
- Schweitzer, G. K., & Pesterfield, L. L. (2010). *The Aqueous Chemistry of the Elements*. Oxford: Oxford University Press. MLA (Modern Language Assoc.) Schweitzer, George Keene and Lester L. Pesterfield
- Shadwick, E. H., Trull, T. W., Thomas, H., & Gibson, J. A. E. (2013). Vulnerability of polar oceans to anthropogenic acidification: comparison of Arctic and Antarctic seasonal cycles. *Scientific reports*, 3, 2339. From <https://www.nature.com/articles/srep02339>
- Stumm, W., & Morgan, J. J. (1996). *Aquatic chemistry: chemical equilibria and rates in natural waters* (Vol. 126). John Wiley & Sons.

- Valverde, J. M., Sanchez-Jimenez, P. E., & Pérez-Maqueda, L. A. (2015). Limestone calcination nearby equilibrium: kinetics, CaO crystal structure, sintering and reactivity. *The Journal of Physical Chemistry C*, 119(4), 1623-1641.
- Völker, C. (2015) Nonlinearities in seawater carbonate chemistry and the distribution of anthropogenic carbon uptake. PowerPoint presentation. Retrieved (29.04.2019): https://epic.awi.de/id/eprint/39020/1/revelle_talk_bremen.pdf
- Wang, S., Yan, S., Ma, X., & Gong, J. (2011). Recent advances in capture of carbon dioxide using alkali-metal-based oxides. *Energy & Environmental Science*, 4(10), 3805-3819.
- Yamamoto-Kawai, M., McLaughlin, F. A., Carmack, E. C., Nishino, S., & Shimada, K. (2009). Aragonite undersaturation in the Arctic Ocean: effects of ocean acidification and sea ice melt. *Science*, 326(5956), 1098-1100.
- Zeebe, R. E., & Wolf-Gladrow, D. (2001). *CO₂ in seawater: equilibrium, kinetics, isotopes* (No. 65). Gulf Professional Publishing.

Appendix A:

Internal and external pH measurements + dataset

Internal measurement is performed inside the tank while external is seawater extracted from the tank and measured in glass beaker stirred with a magnetic stirrer.

Coarse $\sim 0,1 \text{ g CaO L}^{-1}$ seawater:

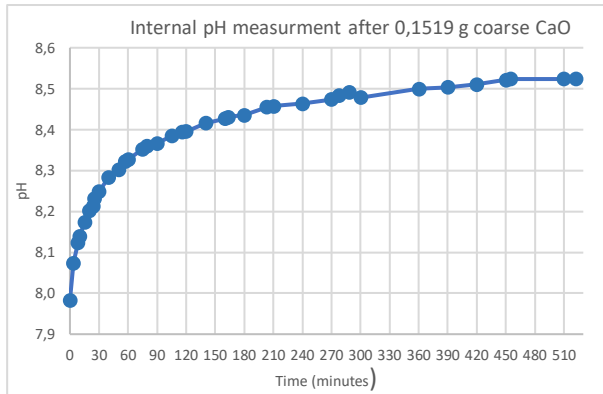


Figure 8: pH meter (A) average slope after calibration: 98,7 %.

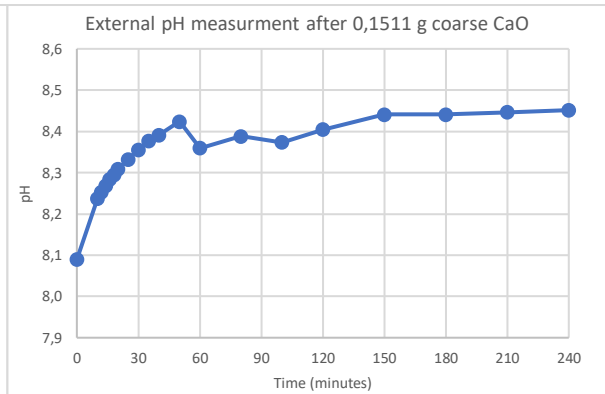


Figure 26: pH meter (A) average slope after calibration: 97,6 %.

Fine $\sim 0,1 \text{ g CaO L}^{-1}$ seawater:

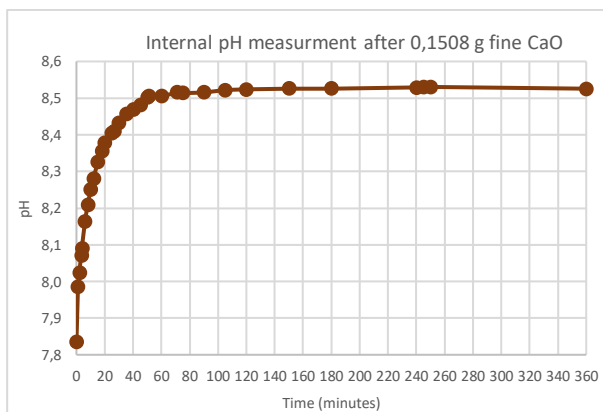


Figure 7: pH meter (A) average slope after calibration: 96,3 %.

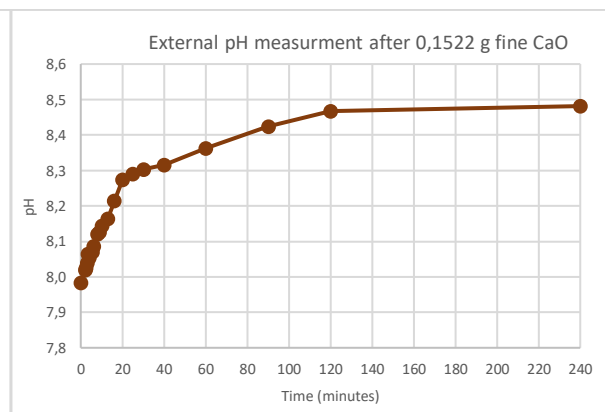


Figure 27: pH meter (A) average slope after calibration: 96,7 %.

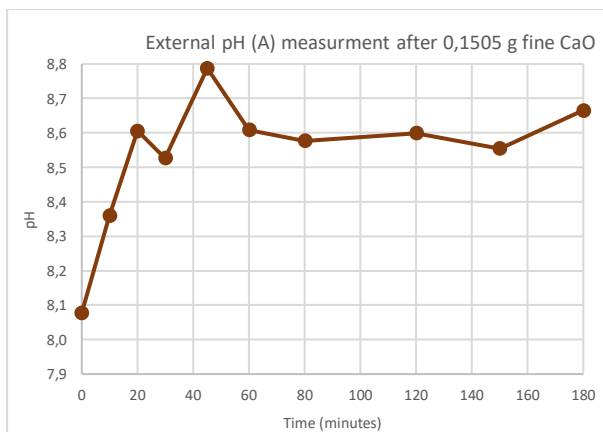


Figure 28: pH meter (A) average slope after calibration: 96,6 %.

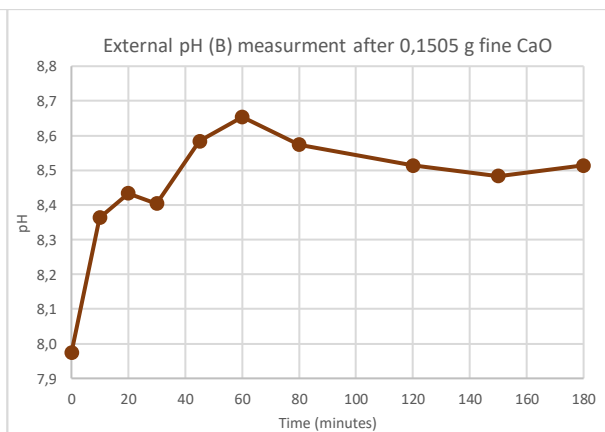


Figure 29: pH meter (B) average slope after calibration: 96,2 %.

Table 3: Dataset figure 8:

| Time (min) | pH | 20 | 8,203 | 57 | 8,322 | 116 | 8,395 | 203 | 8,455 | 300 | 8,479 | 510 | 8,524 |
|------------|-------|----|-------|------|-------|-----|-------|-----|-------|-----|-------|------|-------|
| 0 | 7,984 | 24 | 8,214 | 60 | 8,327 | 120 | 8,396 | 210 | 8,458 | 360 | 8,500 | 522 | 8,524 |
| 3,5 | 8,074 | 25 | 8,232 | 75 | 8,353 | 140 | 8,416 | 240 | 8,464 | 390 | 8,504 | 1240 | 8,534 |
| 8 | 8,124 | 30 | 8,249 | 79,5 | 8,360 | 160 | 8,427 | 270 | 8,474 | 420 | 8,511 | | |
| 10 | 8,140 | 40 | 8,284 | 90 | 8,367 | 163 | 8,431 | 278 | 8,484 | 450 | 8,522 | | |
| 15 | 8,174 | 50 | 8,302 | 105 | 8,385 | 180 | 8,436 | 288 | 8,491 | 455 | 8,524 | | |

Table 4: Dataset figure 7:

| Time (min) | pH | 4 | 8,091 | 15 | 8,326 | 30 | 8,433 | 51 | 8,506 | 105 | 8,522 | 245 | 8,531 |
|------------|-------|----|-------|------|-------|----|-------|----|-------|-----|-------|-----|-------|
| 0 | 7,835 | 6 | 8,164 | 18 | 8,356 | 35 | 8,458 | 60 | 8,506 | 120 | 8,524 | 250 | 8,531 |
| 1 | 7,985 | 8 | 8,210 | 20 | 8,379 | 40 | 8,470 | 71 | 8,516 | 150 | 8,527 | 360 | 8,526 |
| 2 | 8,024 | 10 | 8,251 | 25 | 8,404 | 45 | 8,481 | 75 | 8,514 | 180 | 8,527 | | |
| 3,5 | 8,072 | 12 | 8,281 | 26,5 | 8,410 | 50 | 8,502 | 90 | 8,516 | 240 | 8,529 | | |

Table 5: Dataset figure 11:

| Time (min) | pH | 2 | 8,196 | 5 | 8,308 | 15 | 8,517 | 30 | 8,654 | 60 | 8,756 | 105 | 8,789 |
|------------|-------|---|-------|----|-------|----|-------|----|-------|----|-------|-----|-------|
| 0 | 7,980 | 3 | 8,239 | 7 | 8,361 | 20 | 8,576 | 40 | 8,702 | 75 | 8,772 | 120 | 8,791 |
| 1 | 8,139 | 4 | 8,274 | 10 | 8,432 | 25 | 8,620 | 50 | 8,735 | 90 | 8,783 | 140 | 8,793 |

Table 6: Dataset figure 11:

| Time (min) | pH | 2 | 8,228 | 5 | 8,354 | 15 | 8,593 | 30 | 8,748 | 60 | 8,863 | 107 | 8,902 |
|------------|-------|---|-------|----|-------|----|-------|----|-------|----|-------|-----|-------|
| 0 | 7,954 | 3 | 8,274 | 7 | 8,422 | 20 | 8,659 | 40 | 8,804 | 80 | 8,889 | 120 | 8,905 |
| 1 | 8,152 | 4 | 8,321 | 10 | 8,496 | 25 | 8,711 | 55 | 8,854 | 90 | 8,894 | 140 | 8,906 |

Appendix B:

Dataset for alkalinity and CO₂sys calculation

In the CO₂SYSL EXCEL Macro spreadsheet some variables as salinity (32 ‰), temperature (14 °C), pressure (0 dbar) and pH value at titration endpoint (pH 3,7) are set as constant for all measurements. For determination of alkalinity 1 L of applied seawater is noted to weight 1,026 Kg.

Coarse ~0,1 g CaO L⁻¹ seawater:

Table 7: Average slope for pH electrode (B) used in determine titration endpoint was 95,8 %

| Time | V _{sample} (mL) | V _{0,01 HCl} (mL) | Final pH | Activity coefficient | Total Alkalinity (μmol KgSW ⁻¹) |
|------|--------------------------|----------------------------|----------|----------------------|---|
| 0 | 30,00 | 7,90 | 7,98 | 0,77 | 2363,62 |
| 3,5 | 30,00 | 7,90 | 8,07 | 0,77 | 2363,62 |
| 8 | 30,00 | 7,90 | 8,12 | 0,77 | 2363,62 |
| 15 | 30,00 | 8,00 | 8,17 | 0,77 | 2396,90 |
| 24 | 30,00 | 8,05 | 8,21 | 0,77 | 2413,54 |
| 40 | 30,00 | 8,20 | 8,28 | 0,77 | 2463,47 |
| 57,5 | 30,00 | 8,30 | 8,32 | 0,77 | 2496,75 |
| 90 | 30,00 | 8,30 | 8,37 | 0,77 | 2496,75 |
| 116 | 30,00 | 8,40 | 8,39 | 0,77 | 2530,03 |
| 163 | 30,00 | 8,45 | 8,43 | 0,77 | 2546,67 |
| 203 | 30,00 | 8,50 | 8,45 | 0,77 | 2563,31 |
| 278 | 30,00 | 8,70 | 8,48 | 0,77 | 2629,87 |
| 288 | 30,00 | 8,75 | 8,49 | 0,77 | 2646,51 |
| 360 | 30,00 | 8,70 | 8,50 | 0,77 | 2629,87 |
| 390 | 30,00 | 8,70 | 8,50 | 0,77 | 2629,87 |
| 455 | 30,00 | 8,75 | 8,52 | 0,77 | 2646,51 |
| 522 | 30,00 | 8,75 | 8,52 | 0,77 | 2646,51 |
| 1240 | 30,00 | 8,80 | 8,53 | 0,77 | 2663,15 |

DIC

Table 8: CO₂SYSL EXCEL parameter include NBS scale, pK₁, pK₂ from Mehrbach et al., 1973 refit by Dickson and millero, 1987. KSO₄ source from Dickson and Total Boron source from Uppstrom, 1974. Units for alkalinity, TCO₂, HCO₃⁻, CO₃²⁻, B alk, OH⁻, H⁺ is in μmol kgSW⁻¹.

| Time | Total alkalinity | TCO ₂ | pCO ₂ μatm | Ω Ca | Ω Mg |
|------|------------------|------------------|-----------------------|------|------|
| 0 | 2363,62 | 2232,25 | 660,05 | 2,59 | 1,66 |
| 3,5 | 2363,62 | 2195,68 | 523,02 | 3,11 | 1,99 |
| 8 | 2363,62 | 2173,65 | 458,63 | 3,43 | 2,19 |
| 15 | 2396,90 | 2181,48 | 407,32 | 3,84 | 2,45 |
| 24 | 2413,54 | 2177,02 | 368,36 | 4,17 | 2,67 |
| 40 | 2463,47 | 2185,45 | 310,71 | 4,86 | 3,11 |
| 57,5 | 2496,75 | 2193,82 | 283,50 | 5,28 | 3,38 |
| 90 | 2496,75 | 2166,24 | 249,78 | 5,72 | 3,66 |
| 116 | 2530,03 | 2178,31 | 233,84 | 6,10 | 3,90 |
| 163 | 2546,67 | 2169,18 | 212,27 | 6,53 | 4,18 |
| 203 | 2563,31 | 2167,39 | 199,32 | 6,85 | 4,38 |
| 278 | 2629,87 | 2205,39 | 188,05 | 7,39 | 4,72 |
| 288 | 2646,51 | 2214,85 | 185,42 | 7,52 | 4,81 |
| 360 | 2629,87 | 2193,55 | 179,36 | 7,58 | 4,85 |
| 390 | 2629,87 | 2190,56 | 177,24 | 7,63 | 4,88 |
| 455 | 2646,51 | 2189,98 | 168,09 | 7,94 | 5,08 |
| 522 | 2646,51 | 2189,98 | 168,09 | 7,94 | 5,08 |
| 1240 | 2663,15 | 2196,76 | 164,21 | 8,12 | 5,19 |

Fine ~0,1 g CaO L⁻¹ seawater:

Table 9: Average slope for pH electrode (B) used in determine titration endpoint was 97,6 %

| Time | V _{sample} (mL) | V _{0,01 HCl} (mL) | Final pH | Activity coefficient | Total Alklinity (μmol KgSW ⁻¹) |
|------|--------------------------|----------------------------|----------|----------------------|--|
| 0 | 30,00 | 7,90 | 7,85 | 0,77 | 2363,62 |
| 3,5 | 30,00 | 8,00 | 8,07 | 0,77 | 2396,90 |
| 12 | 30,00 | 8,35 | 8,28 | 0,77 | 2513,39 |
| 18 | 30,00 | 8,45 | 8,36 | 0,77 | 2546,67 |
| 26,5 | 30,00 | 8,50 | 8,41 | 0,77 | 2563,31 |
| 51 | 30,00 | 8,65 | 8,51 | 0,77 | 2613,23 |
| 60 | 30,00 | 8,70 | 8,51 | 0,77 | 2629,87 |
| 71 | 30,00 | 8,70 | 8,52 | 0,77 | 2629,87 |
| 90 | 30,00 | 8,80 | 8,52 | 0,77 | 2663,15 |
| 105 | 30,00 | 8,80 | 8,52 | 0,77 | 2663,15 |
| 150 | 30,00 | 8,80 | 8,53 | 0,77 | 2663,15 |
| 245 | 30,00 | 8,85 | 8,53 | 0,77 | 2679,79 |
| 250 | 30,00 | 8,80 | 8,53 | 0,77 | 2663,15 |
| 360 | 30,00 | 8,80 | 8,53 | 0,77 | 2663,15 |

Table 10: CO2SYS EXCEL parameter include NBS scale, pK1, pK2 from Mehrbach et al., 1973 refit by Dickson and millero, 1987. KSO4 source from Dickson and Total Boron source from Uppstrom, 1974. Units for alkalinity, TCO2, HCO3-, CO32-, B alk, OH-, H+ is in μmol kgSW-1.

| Time | Total alkalinity | TCO ₂ | pCO ₂ μatm | Ω Ca | Ω Mg |
|------|------------------|------------------|-----------------------|------|------|
| 0 | 2363,62 | 2279,32 | 916,94 | 1,98 | 1,27 |
| 3,5 | 2396,90 | 2228,25 | 533,35 | 3,14 | 2,01 |
| 12 | 2513,39 | 2233,10 | 319,88 | 4,93 | 3,15 |
| 18 | 2546,67 | 2218,37 | 263,04 | 5,73 | 3,66 |
| 26,5 | 2563,31 | 2198,25 | 227,07 | 6,34 | 4,06 |
| 51 | 2613,23 | 2174,50 | 175,02 | 7,61 | 4,86 |
| 60 | 2629,87 | 2189,07 | 176,19 | 7,66 | 4,90 |
| 71 | 2629,87 | 2181,54 | 171,02 | 7,78 | 4,98 |
| 90 | 2663,15 | 2210,60 | 173,30 | 7,89 | 5,04 |
| 105 | 2663,15 | 2206,01 | 170,22 | 7,97 | 5,09 |
| 150 | 2663,15 | 2202,17 | 167,69 | 8,03 | 5,13 |
| 245 | 2679,79 | 2213,56 | 166,78 | 8,14 | 5,20 |
| 250 | 2663,15 | 2199,08 | 165,69 | 8,08 | 5,17 |
| 360 | 2663,15 | 2202,94 | 168,20 | 8,02 | 5,13 |

Appendix D:

ICP-MS dataset and Ca/Mg correlation

Three blank samples were prepared by pressing Milli-Q water through the Sartobran® Capsule 0.2 µm filter with a syringe. The difference in value are however a bit alarming and should be taken into consideration when validating the other samples.

| | Mg25 µg/L | RSD, % | Ca44 µg/L | RSD, % |
|--------------|-----------|--------|-----------|--------|
| Blank sample | 380 166 | 2,3 | 121 930 | 2,7 |
| Blank sample | 200 198 | 1,3 | 63 916 | 1,6 |
| Blank sample | 504 787 | 1,2 | 163 252 | 2,7 |

Table 13: Ca and Mg content after 0,1516 g coarse CaO

| Timen (min) | Ca44 µg/L | RSD | Mg25 µg/L | RSD |
|-------------|-----------|---------|------------|---------|
| 0 | 395153,65 | 5,92 % | 1235279,79 | 4,98 % |
| 15 | 429552,77 | 1,80 % | 1319357,66 | 3,16 % |
| 30 | 416660,17 | 2,79 % | 1300371,00 | 2,12 % |
| 45 | 419615,99 | 4,55 % | 1289477,81 | 4,02 % |
| 60 | 407377,62 | 1,40 % | 1279498,61 | 0,80 % |
| 75 | 417474,33 | 2,30 % | 1279600,49 | 2,67 % |
| 90 | 421470,23 | 3,23 % | 1305820,51 | 2,73 % |
| 105 | 419030,15 | 3,33 % | 1295397,79 | 3,40 % |
| 120 | 429973,03 | 3,61 % | 1319289,60 | 3,38 % |
| 135 | 415482,47 | 3,78 % | 1277833,39 | 3,43 % |
| 150 | 423486,06 | 4,50 % | 1322575,68 | 3,24 % |
| 165 | 419747,64 | 3,88 % | 1266680,40 | 3,97 % |
| 180 | 431701,15 | 2,63 % | 1300227,21 | 2,17 % |
| 195 | 423183,94 | 3,47 % | 1278628,87 | 1,42 % |
| 210 | 408213,85 | 5,67 % | 1265501,33 | 2,67 % |
| 225 | 414444,69 | 3,53 % | 1261848,99 | 3,35 % |
| 240 | 376338,00 | 18,20 % | 1153201,25 | 17,00 % |
| 255 | 414076,06 | 3,49 % | 1265861,08 | 6,32 % |
| 270 | 417893,41 | 2,19 % | 1268718,16 | 4,30 % |
| 285 | 420001,02 | 3,58 % | 1285729,63 | 4,96 % |
| 300 | 418113,41 | 2,17 % | 1276725,21 | 2,47 % |

Table 17: Ca and Mg content after 0,1502 g fine CaO

| Timen (min) | Ca44 µg/L | RSD | Mg25 µg/L | RSD |
|-------------|-----------|--------|-------------|--------|
| 0 | 395153,65 | 5,92 % | 1235279,794 | 4,98 % |
| 10 | 414615,20 | 4,87 % | 1280227,334 | 2,21 % |
| 20 | 421665,14 | 5,96 % | 1268992,473 | 3,82 % |
| 30 | 415395,89 | 3,56 % | 1268222,632 | 7,32 % |
| 40 | 423124,70 | 4,44 % | 1277687,766 | 3,04 % |
| 50 | 416851,78 | 6,32 % | 1287151,109 | 3,83 % |
| 60 | 416670,06 | 4,80 % | 1289698,725 | 5,14 % |
| 70 | 409270,45 | 3,04 % | 1254639,283 | 4,44 % |
| 80 | 409210,32 | 3,29 % | 1271629,676 | 5,80 % |
| 90 | 418092,07 | 3,95 % | 1281823,122 | 3,29 % |
| 100 | 408712,93 | 5,23 % | 1253560,917 | 5,72 % |
| 110 | 433108,12 | 4,78 % | 1282139,21 | 5,43 % |
| 120 | 410238,64 | 4,86 % | 1242608,496 | 6,29 % |
| 130 | 414212,18 | 6,58 % | 1256195,689 | 7,09 % |
| 140 | 411565,07 | 3,55 % | 1262960,927 | 4,73 % |
| 150 | 418151,60 | 6,49 % | 1269970,724 | 5,45 % |
| 160 | 418066,42 | 4,80 % | 1269773,135 | 6,61 % |
| 170 | 415852,57 | 5,93 % | 1253451,641 | 4,29 % |
| 180 | 410505,45 | 4,53 % | 1253204,014 | 5,64 % |
| 190 | 410221,83 | 4,03 % | 1255059,526 | 2,91 % |
| 200 | 414803,43 | 5,36 % | 1269651,829 | 3,26 % |

Table 18: Ca and Mg content after 0,2252 g fine CaO

| Timen (min) | Ca44 µg/L | RSD | Mg25 µg/L | RSD |
|-------------|-----------|---------|------------|--------|
| 0 | 395153,65 | 5,92 % | 1235279,79 | 4,98 % |
| 10 | 407337,10 | 2,94 % | 1260457,59 | 6,17 % |
| 20 | 428056,34 | 3,62 % | 1304528,29 | 4,68 % |
| 30 | 410632,10 | 2,93 % | 1283684,82 | 6,00 % |
| 40 | 422462,17 | 4,08 % | 1298601,02 | 3,43 % |
| 50 | 413996,83 | 5,58 % | 1263571,45 | 3,73 % |
| 60 | 415892,38 | 5,36 % | 1279288,05 | 6,28 % |
| 70 | 413925,47 | 5,09 % | 1265764,32 | 5,85 % |
| 80 | 415195,07 | 5,18 % | 1250707,87 | 4,87 % |
| 90 | 417271,62 | 4,00 % | 1272843,13 | 4,08 % |
| 100 | 418611,64 | 3,23 % | 1273827,64 | 2,59 % |
| 110 | 429859,77 | 3,42 % | 1286067,38 | 4,53 % |
| 120 | 422913,18 | 5,08 % | 1269580,13 | 5,12 % |
| 130 | 419982,28 | 7,65 % | 1268922,37 | 7,38 % |
| 140 | 415803,87 | 5,03 % | 1280762,88 | 3,23 % |
| 150 | 407576,41 | 8,12 % | 1246291,81 | 3,57 % |
| 160 | 413888,93 | 6,22 % | 1262967,73 | 3,84 % |
| 170 | 422447,29 | 6,62 % | 1275716,94 | 1,95 % |
| 180 | 413299,55 | 4,44 % | 1265417,28 | 5,60 % |
| 190 | 406428,32 | 7,06 % | 1252919,71 | 8,33 % |
| 200 | 424971,97 | 10,35 % | 1305039,94 | 8,98 % |

Table 19: Ca and Mg content after 0,3002 g fine CaO

| Timen (min) | Ca44 µg/L | RSD | Mg25 µg/L | RSD |
|-------------|-----------|---------|------------|---------|
| 0 | 395153,65 | 5,92 % | 1235279,79 | 4,98 % |
| 10 | 413963,76 | 4,50 % | 1286638,23 | 5,10 % |
| 20 | 388422,06 | 19,76 % | 1192063,31 | 18,26 % |
| 30 | 412400,24 | 3,69 % | 1265963,97 | 4,85 % |
| 40 | 422634,79 | 5,59 % | 1297686,64 | 6,22 % |
| 50 | 427083,03 | 5,10 % | 1292953,60 | 4,66 % |
| 60 | 416579,29 | 3,62 % | 1288361,46 | 3,74 % |
| 70 | 430286,20 | 5,86 % | 1306861,30 | 4,56 % |
| 80 | 419108,82 | 3,74 % | 1263501,42 | 5,49 % |
| 90 | 421423,84 | 4,69 % | 1301274,38 | 3,35 % |
| 100 | 405939,26 | 5,10 % | 1230555,52 | 2,83 % |
| 110 | 419017,56 | 4,36 % | 1287440,60 | 5,18 % |
| 120 | 425719,91 | 3,55 % | 1302446,31 | 1,31 % |
| 130 | 436165,67 | 3,70 % | 1326370,78 | 3,67 % |
| 140 | 427559,40 | 4,82 % | 1301176,88 | 4,44 % |
| 150 | 435088,52 | 4,47 % | 1329101,06 | 5,93 % |
| 160 | 442371,18 | 3,56 % | 1350430,81 | 2,94 % |
| 170 | 449982,56 | 2,74 % | 1372538,80 | 1,95 % |
| 180 | 420572,85 | 4,25 % | 1283253,33 | 2,03 % |
| 190 | 422618,35 | 3,40 % | 1301842,04 | 2,04 % |
| 200 | 426553,62 | 1,89 % | 1301192,07 | 2,93 % |

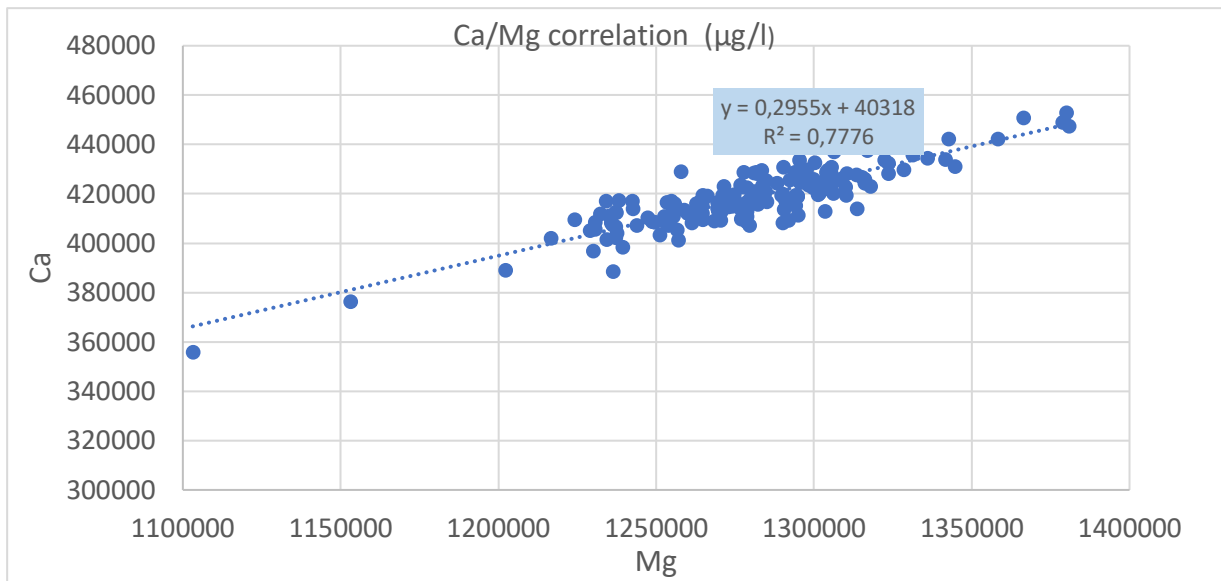


Figure 30: Ca/Mg correlation are strong even though only Ca is added to the solution. Figure from Syverin Lierhagen.

Appendix E:

Dataset from PIC determination

Filter IR analyses of carbon and nitrogen was performed by Kjersti Andresen from Trondheim Biological Station (TBS). CO₂ (g) and NO_x (g) is measured when the samples are heated up. The GFF filters packed in tinfoil had to be divided and repacked at one point when it was discovered they might be stuck during analyses. The two subsamples from each sample was then added together in the data presented in this study.

The result presented in table 20 for organic reference is deviating and problematic for concluding organic behaviour in sample. An apparent doubt for the reference results credibility comes from observation of the tinfoil around the samples being “burned”. The tinfoil would then only cover the samples sporadically and big parts of the filters left open for soundings.

Table 20: Organic references taken from 0,1505 g fine CaO mixed with 15 L seawater, 1 atm. Samples at 0,90,180 minutes taken in the same run-through as for XRF, Table 12 and 13 and figure 21 and 22. Samples was treated to acid fume from 0,1 M HNO₃ for 6 hours before being packed by tinfoil and stored in a desiccator. Time between sample collecting and analyse was approximately 4 and a half months.

| Time | Reference | µg N/capsule | µg C/capsule | Comment |
|------|-----------|--------------|--------------|---|
| 0 | 21A | 8,19 | 35,36 | |
| 0 | 21B | 5,36 | 23,16 | |
| 0 | 21C | 18,65 | 393,29 | High values for both 21C(A) (305) and 21C(B) (88) |
| 90 | 22A | 12,73 | 34,42 | |
| 90 | 22B | 5,87 | 17,76 | |
| 90 | 22C | 3,34 | 15,18 | |
| 180 | 23A | 10,50 | 235,04 | High values for both 23A(A) (193) and 23A(B) (42) |
| 180 | 23B | 12,32 | 250,37 | High values for both 23B(A) (196) and 23B(B) (54) |
| 180 | 23C | 5,08 | 20,37 | |

Table 21: N/C content in GFF filtrated with 200 mL seawater sample after addition of 0,1516 g coarse CaO in 15 L seawater

| Time | µg N/capsule | µg C/capsule | N ± | C ± | Comment |
|------|--------------|--------------|------|-------|--|
| 0 | 3,40 | 25,69 | 0,87 | 2,40 | |
| 15 | 3,92 | 36,20 | 0,81 | 4,71 | |
| 30 | 3,03 | 31,46 | 0,19 | 1,94 | |
| 45 | 3,46 | 31,30 | 0,57 | 0,37 | |
| 60 | 5,45 | 26,59 | 0,20 | 1,27 | |
| 75 | 3,77 | 29,05 | 0,17 | 2,38 | |
| 90 | 3,27 | 24,78 | 0,46 | 3,95 | |
| 105 | 2,92 | 21,59 | 0,10 | 0,48 | |
| 120 | 3,46 | 29,93 | 0,77 | 0,08 | |
| 135 | 3,92 | 21,54 | 0,65 | 0,98 | |
| 150 | 3,81 | 22,93 | 1,32 | 1,53 | |
| 165 | 12,09 | 78,19 | 6,59 | 52,68 | Large deviance (120) in subsample 11B(B) |
| 180 | 5,05 | 28,47 | 1,97 | 0,94 | |
| 195 | 3,19 | 15,84 | | | Data from 13A. No duplicate |
| 210 | 3,57 | 24,71 | 0,47 | 1,47 | |
| 225 | 2,92 | 22,16 | 0,25 | 1,49 | |
| 240 | 4,35 | 25,87 | 0,17 | 1,33 | |
| 255 | 2,90 | 29,23 | 1,23 | 2,94 | |
| 270 | 2,49 | 30,20 | 0,41 | 3,13 | |
| 285 | 2,89 | 32,13 | 0,68 | 7,31 | |
| 300 | 6,19 | 25,28 | | | Data from 20B. No duplicate |

Table 22: N/C content in GFF filtrated with 200 mL seawater sample after addition of 0,1502 g fine CaO in 15 L seawater

| Time | µg N/capsule | µg C/capsule | N ± | C ± | Comment |
|------|--------------|--------------|------|-------|-----------------------------|
| 0 | 1,07 | 20,65 | 0,87 | 1,47 | |
| 10 | 3,30 | 100,01 | 0,16 | 30,39 | |
| 20 | 2,39 | 73,39 | 0,11 | 8,78 | |
| 30 | 2,44 | 59,05 | 0,63 | 5,26 | |
| 40 | 2,32 | 53,82 | 0,07 | 8,96 | |
| 50 | 2,11 | 41,42 | 0,02 | 1,48 | |
| 60 | 3,38 | 41,65 | 0,25 | 0,65 | |
| 70 | 3,06 | 43,34 | 1,44 | 0,76 | |
| 80 | 2,51 | 34,17 | 0,07 | 4,11 | |
| 90 | 2,11 | 28,47 | 0,24 | 0,57 | |
| 100 | 2,75 | 27,87 | 0,62 | 1,46 | |
| 110 | 2,42 | 27,90 | 0,00 | 1,03 | |
| 120 | 1,87 | 27,74 | 0,19 | 4,52 | |
| 130 | 3,10 | 23,28 | 1,23 | 2,29 | |
| 140 | 3,05 | 27,67 | 0,99 | 1,19 | |
| 150 | 3,57 | 29,88 | 1,28 | 0,31 | |
| 160 | 1,62 | 30,75 | 0,35 | 0,43 | |
| 170 | 1,34 | 28,18 | | | Data from 17A. No duplicate |
| 180 | 1,58 | 35,02 | 0,28 | 0,06 | |
| 190 | 2,67 | 51,42 | 0,29 | 4,44 | |
| 200 | 2,20 | 33,52 | 0,40 | 0,54 | |

Table 23: N/C content in GFF filtrated with 200 mL seawater sample after addition of 0,2252 g fine CaO in 15 L seawater


| Time | µg N/capsule | µg C/capsule | N ± | C ± | Comment |
|------|--------------|--------------|------|-------|-----------------------------|
| 0 | 1,07 | 20,65 | 0,87 | 1,47 | |
| 10 | 1,93 | 130,63 | 0,41 | 2,20 | |
| 20 | 1,95 | 67,70 | 1,33 | 30,17 | |
| 30 | 1,04 | 48,09 | 0,24 | 1,52 | |
| 40 | 2,54 | 41,75 | 0,38 | 7,99 | |
| 50 | 1,94 | 35,32 | 0,85 | 3,09 | |
| 60 | 1,71 | 37,12 | 0,06 | 3,25 | |
| 70 | 2,04 | 40,81 | 1,09 | 2,79 | |
| 80 | 2,15 | 34,09 | 0,48 | 1,74 | |
| 90 | 1,37 | 31,43 | 0,34 | 0,05 | |
| 100 | 1,58 | 33,85 | 0,08 | 1,47 | |
| 110 | 1,18 | 37,19 | 1,17 | 1,71 | |
| 120 | 0,61 | 34,47 | | | Data from 12A. No duplicate |
| 130 | 1,19 | 33,19 | 0,60 | 4,10 | |
| 140 | 0,99 | 32,92 | 0,47 | 2,60 | |
| 150 | 0,88 | 31,90 | | | Data from 15B. No duplicate |
| 160 | 2,12 | 29,82 | 0,11 | 0,32 | |
| 170 | 0,86 | 30,73 | 0,43 | 7,08 | |
| 180 | 1,01 | 33,45 | 0,20 | 3,99 | |
| 190 | 1,93 | 31,70 | 0,26 | 1,60 | |
| 200 | 1,18 | 33,44 | 0,09 | 3,09 | |

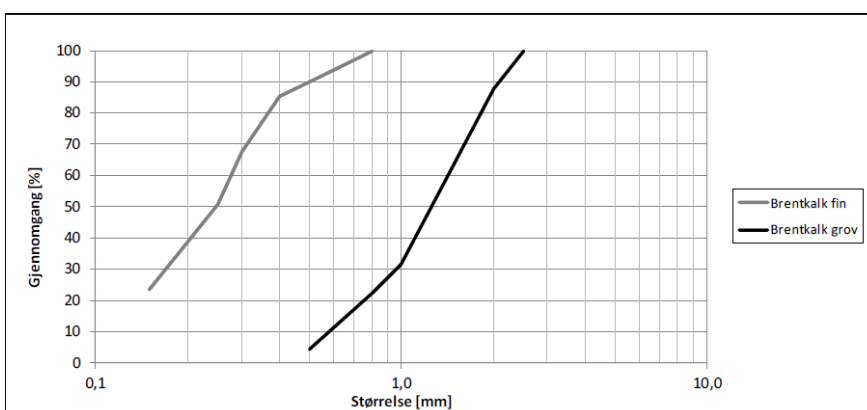
Table 24: N/C content in GFF filtrated with 200 mL seawater sample after addition of 0,3002 g fine CaO in 15 L seawater

| Time | µg N/capsule | µg C/capsule | N ± | C ± | Comment |
|------|--------------|--------------|------|-------|-----------------------------|
| 0 | 1,07 | 20,65 | 0,87 | 1,47 | |
| 10 | 1,71 | 208,10 | 0,48 | 13,29 | |
| 20 | 2,14 | 134,80 | 0,90 | 14,89 | |
| 30 | 2,04 | 110,84 | 0,10 | 9,64 | |
| 40 | 1,06 | 79,36 | 0,48 | 7,91 | |
| 50 | 1,30 | 74,39 | 0,39 | 0,41 | |
| 60 | 0,87 | 62,53 | 0,25 | 5,55 | |
| 70 | 1,06 | 55,58 | 0,02 | 7,50 | |
| 80 | 1,12 | 43,77 | 0,50 | 0,32 | |
| 90 | 2,42 | 43,42 | 0,80 | 5,81 | |
| 100 | 1,08 | 36,40 | 0,02 | 1,77 | |
| 110 | 1,13 | 40,02 | 0,99 | 4,04 | |
| 120 | 0,93 | 48,37 | 0,10 | 8,07 | |
| 130 | 0,40 | 37,02 | 0,38 | 1,84 | |
| 140 | 0,42 | 37,77 | 0,05 | 0,10 | |
| 150 | 1,13 | 40,74 | 0,53 | 4,66 | |
| 160 | 0,42 | 37,51 | 0,04 | 1,81 | |
| 170 | 1,94 | 44,68 | | | Data from 17A. No duplicate |
| 180 | 0,67 | 44,28 | 0,31 | 0,88 | |
| 190 | 1,22 | 40,38 | 0,64 | 0,03 | |
| 200 | | | | | Missing data |

Appendix F:

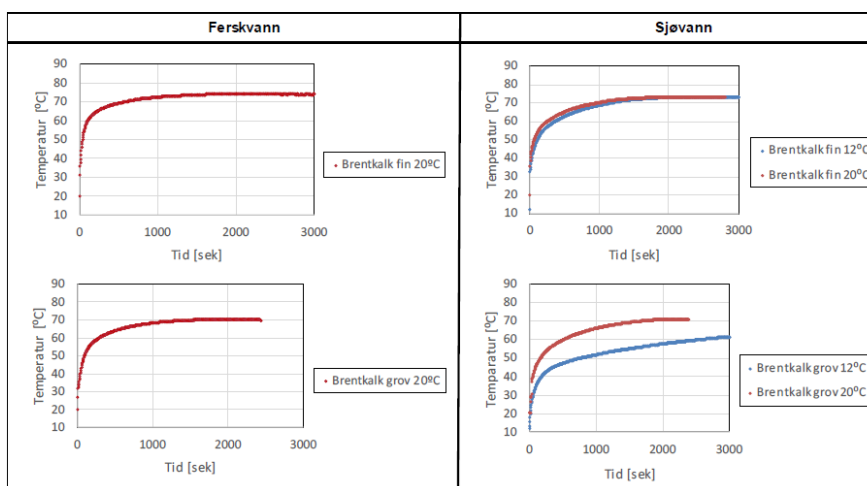
Analyserapport AR-MKA-17-0030 fra Miljøkalk AS

| Analyserapport (AR-MKA-17-0030) | | | | | |
|------------------------------------|--|---------------------|--|---|--------------------------------|
| Produkt : | Prøvemateriale til prosjekt "Brentkalk i sjøvann" Brentkalk fin Oppd-002236 Brentkalk grov Oppd-002237 | | | Miljøkalk AS Olav Ingstadsvei 5 NO-1309 Rud Telefon: +47 05255 | |
| Analyse: | Metode | Basert på |  Analyserapport nr: 17-0030 Oppdragsgiver : MKA Dato : 20.09.17 Forfatter : Kjell R. Kvam Status: intern | | |
| | CaO-aktiv | Internt | ASTM C25-11 E1 | | |
| | Leco | Internt | ASTM C25-11 | | |
| | Halogen tørvekt | Internt | ASTM C25-11 E1 | | |
| | Sikting | Internt | NS-EN 933-1 | | |
| | Reaktivitet | Internt | NS-EN 459-2 | | |
| | Spesifisk overflate | Internt | BET | | |
| Metode | Parameter | Enhet | Brentkalk fin | Brentkalk grov | Kommentar |
| CaO-aktiv | CaO | [%] | 94* | 91* | Analyser med nedmalt fraksjon* |
| Leco | CO ₂ -rest | [%] | 1,6* | 2,7* | |
| Halogen tørvekt | Vanninnhold | [%] | <0,1 | <0,1 | |
| Spesifisk overflate | BET | [m ² /g] | 1,53 | 1,12 | |
| Sikting | 0,2 mm | [%] | 24 | - | |
| | 0,3 mm | [%] | 51 | - | |
| | 0,3 mm | [%] | 68 | - | |
| | 0,4 mm | [%] | 85 | - | |
| | 0,5 mm | [%] | 90 | 4 | |
| | 0,8 mm | [%] | 100 | 23 | |
| | 1,0 mm | [%] | - | 32 | |
| | 2,0 mm | [%] | - | 88 | |
| | 2,5 mm | [%] | - | 100 | |
| Siktekurve | | | | | |



| Reaktivitet | | | Brentkalk fin | Brentkalk grov | Kommentar |
|-------------|------------|-------|---------------|----------------|-----------|
| Ferskvann | t60°C* | [sek] | 100 | 250 | |
| | dT totalt* | [°C] | 75 | 75 | |
| Sjøvann | t60°C* | [sek] | 300 | 500 | |
| | dT totalt* | [°C] | 70 | 70 | |

Leskekurve*



20.09.17
Dato

Kjell R. Kvam
Godkjent

